# High Weissenberg number boundary layer structures for Phan-Thien-Tanner fluids

J.D. Evans*
Department of Mathematical Sciences, University of Bath,
Bath BA2 7AY, United Kingdom

July 2005

**Abstract**

We describe here the boundary layer structures that can arise in high Weissenberg number flows for Phan-Thien-Tanner (PTT) fluids. The model is considered in the absence of solvent stresses and it is shown that the type of boundary layer structure depends upon the size of the PTT model parameter $\kappa$. In $\kappa = O(1)$ flows, only one structure is possible whilst in $\kappa = o(1)$ flows a far richer variety of balances and consequent structures arise. Central to all structures will be regions where one of three distinct balances within the constitutive equations dominate. These three balances represent the three distinct viscometric behaviours PTT fluids can posses in high Weissenberg number flows and arise according to the relative sizes of $\kappa$ and the Weissenberg number. The structures considered here are complete in the sense that they describe the smooth transition between PTT $\kappa = O(1)$ boundary layers and the upper convected Maxwell (UCM) boundary layers obtained when $\kappa = 0$.

*Key words and phrases: Phan-Thien-Tanner fluid; high Weissenberg number; boundary layers*

* e-mail: masjde@maths.bath.ac.uk

# 1. Introduction

High Weissenberg number flows are a singular limit in which the elastic effects of model equations are usually most pronounced. This has been seen in [6] and [1] for the upper convected Maxwell (UCM) model, where boundary layers are shown to form at solid walls. Here we continue this analysis for Phan-Thien-Tanner (PTT) fluids, extending the previous work of [3].

The PTT fluid model is an extension of the UCM model, where a quadratic stress term is added to the constitutive law (see [5]). Such a term is included in order to correct the UCM model's over prediction of stresses at large deformation rates. As explained in [8], the PTT model is successful at capturing shear thinning effects and reduction in first normal stress difference with increased shear rates associated with real polymeric fluids. [1] The dimensionless governing equations that we consider are the usual momentum and continuity equations

$$\mathrm{Re}\,\mathbf{v}\cdot\nabla\mathbf{v} = -\nabla p + \nabla\cdot\mathbf{T}, \qquad \nabla\cdot\mathbf{v} = 0, \tag{1.1}$$

together with the PTT constitutive equations

$$\mathbf{T} + \mathrm{We}\left(\overset{\triangledown}{\mathbf{T}} + \kappa(\mathrm{tr}\mathbf{T})\mathbf{T}\right) = 2\mathbf{D}, \tag{1.2}$$

where $\mathbf{v}$ is the velocity, $p$ is the pressure, $\mathbf{T}$ is the extra-stress tensor, $\overset{\triangledown}{\mathbf{T}}$ is the upper convected stress derivative and $\mathbf{D} = \frac{1}{2}(\nabla\mathbf{v} + (\nabla\mathbf{v})^T)$ is the rate of strain tensor. The dimensionless parameters are the Weissenberg number We, the Reynolds number Re and the PTT model parameter $\kappa$. We are interested in describing the high Weissenberg limit $\mathrm{We}\to\infty$, with the Reynolds number and PTT model parameter generally assumed to be order one. Here, the Reynolds number controls the influence of the inertia terms within the momentum equations whilst the PTT model parameter controls the influence of the quadratic stress terms in the constitutive equations. As terminology, we will refer to the first term in (1.2) as the linear stress term and the third term as the quadratic stress term. It is important to note that we do not include the presence of a Newtonian solvent stress in the momentum equation, and as such we are here only considering flows with vanishingly small Newtonian viscosity.

In the high Weissenberg limit, we expect the upper convected stress derivative and quadratic stress terms in (1.2) to dominate in regions away from the walls. The flows in such regions will be termed core flows and represent outer regions in the terminology of matched asymptotic expansions. This immediately gives two balances to consider for such regions depending upon the size of $\kappa$. When $\kappa = O(1)$ the quadratic stress terms are significant and we have $\overset{\triangledown}{\mathbf{T}} + \kappa(\mathrm{tr}\mathbf{T})\mathbf{T} = 0$ at leading order in We, whilst if $\kappa = o(1)$ then the quadratic stress terms are negligible and we obtain instead $\overset{\triangledown}{\mathbf{T}} = 0$. The main aim of this paper is to classify the boundary layer structures that can accommodate such core flow balances.

Crucial to understanding possible boundary layer balances (i.e. the balances between the terms in (1.2) in narrow regions at solid boundaries) is the determination of viscometric (i.e. simple shear flow) behaviour for the constitutive equations. Since such behaviour must occur

[1] Nevertheless, a zero second normal stress difference is still obtained. This is corrected in the Giesekus model [2], which is another popular constitutive model that adds a quadratic stress term to the UCM equations. However, the form of such a term for this model is sufficiently different to change the analysis from that for the PTT equations and needs separate consideration from that given here.

at solid boundaries when the no-slip condition is imposed, understanding viscometric behaviour gives the important information as to which omitted terms in (1.2) need to be recovered. As we shall see, this depends critically upon the size of $\kappa$.

The layout of the paper is as follows. In section 2, viscometric behaviour is investigated and the important balances within (1.2) identified. In section 3, the $\kappa = O(1)$ flows are considered, so that we only have one small parameter in the problem, namely $\mathrm{We}^{-1}$. Here it is shown that there is only one set of boundary layer equations of general significance. For these equations, the wall behaviour and core matching conditions are derived. As regards the latter, solutions in separable form are obtained for general limiting core behaviour. In section 4 the $\kappa = o(1)$ flows are considered. Now the problem has two small parameters, namely $\kappa$ and $\mathrm{We}^{-1}$, and consequently we show that a rich variety (nine distinct types) of boundary layer structures is possible. These may be identified according to the relative sizes of $\kappa$ and $\mathrm{We}^{-1}$ (there being the three cases $0 < r < 1, r = 1, r > 1$ if $\kappa = O(\mathrm{We}^{-r})$) and for each of these cases three ranges for the limiting core behaviour. These structures explain the transition from the $\kappa = O(1)$ boundary layer of section 3 through to the UCM boundary layer equations that occur when $\kappa = 0$.

As regards previous work, the viscometric behaviour and two main single layer balances were identified in [3]. Essentially, these are put in context here through consideration of matching with core flow behaviour and the boundary layer description completed by identifying possible double layer structures.

## 2. Viscometric behaviour

In component form, (1.2) is

$$T_{11} + \mathrm{We}\left(\frac{\partial\psi}{\partial y}\frac{\partial T_{11}}{\partial x} - \frac{\partial\psi}{\partial x}\frac{\partial T_{11}}{\partial y} - 2\frac{\partial^2\psi}{\partial y^2}T_{12} - 2\frac{\partial^2\psi}{\partial x\partial y}T_{11} + \kappa T_{11}(T_{11}+T_{22})\right) = 2\frac{\partial^2\psi}{\partial x\partial y}, \quad (2.1)$$

$$T_{22} + \mathrm{We}\left(\frac{\partial\psi}{\partial y}\frac{\partial T_{22}}{\partial x} - \frac{\partial\psi}{\partial x}\frac{\partial T_{22}}{\partial y} + 2\frac{\partial^2\psi}{\partial x^2}T_{12} + 2\frac{\partial^2\psi}{\partial x\partial y}T_{22} + \kappa T_{22}(T_{11}+T_{22})\right) = -2\frac{\partial^2\psi}{\partial x\partial y}, \quad (2.2)$$

$$T_{12} + \mathrm{We}\left(\frac{\partial\psi}{\partial y}\frac{\partial T_{12}}{\partial x} - \frac{\partial\psi}{\partial x}\frac{\partial T_{12}}{\partial y} + \frac{\partial^2\psi}{\partial x^2}T_{11} - \frac{\partial^2\psi}{\partial y^2}T_{22} + \kappa T_{12}(T_{11}+T_{22})\right) = \frac{\partial^2\psi}{\partial y^2} - \frac{\partial^2\psi}{\partial x^2}. \quad (2.3)$$

We now consider steady shear flow in which the stream function takes the general theoretical form

$$\psi = \frac{1}{2}\dot{\gamma}y^2\mathrm{We}^{-\frac{(m-2)}{2}}. \quad (2.4)$$

Here $\dot{\gamma} = O(1)$ and the exponent $m$ is at our disposal (the particular form of its occurrence following that adopted for the UCM case $\kappa = 0$ (see [1]) i.e. the exponent $m$ has been chosen so that an order one shear rate is obtained when $m = 2$ and $T_{11} = O(1)$ when $m = 3$ for the limit $\mathrm{We} \to \infty$ when $\kappa = 0$).

For the region $y = O(1)$, we are thus considering a Weissenberg dependent shear rate $\dot{\gamma}\mathrm{We}^{-\frac{(m-2)}{2}}$. The main reason for its introduction is that we wish to focus on situations in which the extra stress component $T_{11}$ is order one. As we shall see in the subsequent sections, it this scaling that is important within the boundary layer structures since it allows the pressure gradient (which does not vary across the boundary layer width) to be maintained at leading order. The implication of (2.4) is that an order one shear rate in steady shear flow now occurs at distances $O(\mathrm{We}^{\frac{(m-2)}{4}})$ from the wall. If $m \neq 2$, then this length scale will differ from the order one length scales on which the dimensionless equations (2.1)–(2.3) are assumed to hold (and will be comparatively closer to the wall for $m < 2$ and farther from the wall for $m > 2$). The most common situation experimentally is that these two length scales coincide i.e. $m = 2$. For them to be different, clearly requires the use of a characteristic time scale for nondimensionalisation that differs from both the dimensional relaxation time of the fluid and the dimensional wall shear rate. It is not clear at this stage if such a flow can be created experimentally, in which case the introduction of such a characteristic time scale may only be a convenient theoretical artifact to allow steady shear flow to reproduce the scalings obtained later for the single boundary layer structures. The characteristic time scale would necessarily need to be obtained from flow in a region external to that considered here e.g. through the use of characteristic length and velocity scale applicable in another part of the flow domain. Whether we can consider $m$ different from 2 or not experimentally, it is still of benefit to consider the theoretical form (2.4) due to its ability to recreate the scalings for the non-zero extra stress components that we will find later for the single boundary layer structures.

Using (2.4), the equations (2.1)–(2.3) then give

$$T_{11} + \mathrm{We}\left(-2\dot{\gamma}\mathrm{We}^{-\frac{(m-2)}{2}}T_{12} + \kappa T_{11}(T_{11}+T_{22})\right) = 0, \tag{2.5}$$

$$T_{22} + \mathrm{We}\left(\kappa T_{22}(T_{11}+T_{22})\right) = 0, \tag{2.6}$$

$$T_{12} + \mathrm{We}\left(-\dot{\gamma}\mathrm{We}^{-\frac{(m-2)}{2}}T_{22} + \kappa T_{12}(T_{11}+T_{22})\right) = \dot{\gamma}\mathrm{We}^{-\frac{(m-2)}{2}}, \tag{2.7}$$

which are the equations derived in [3], allowing for this more general shear rate. Provided $\mathrm{We}\kappa T_{11} \neq -1$ then these equations may be solved to give

$$T_{22} = 0, \qquad T_{11} = 2\mathrm{We}T_{12}^2,$$

with $T_{12}$ satisfying

$$T_{12} + 2\mathrm{We}^2\kappa T_{12}^3 = \dot{\gamma}\mathrm{We}^{-\frac{(m-2)}{2}}, \tag{2.8}$$

or equivalently $T_{11}$ satisfying

$$T_{11}(1+\mathrm{We}\kappa T_{11})^2 = 2\dot{\gamma}^2\mathrm{We}^{3-m}. \tag{2.9}$$

We now take the limit $\mathrm{We} \to \infty$ and distinguish several cases depending on the size of $\kappa$. For the moment, the exponent $m$ may be considered fixed and restricted to the range $m < 4$.

(a) For $\kappa = O(1)$ we have

$$T_{11} \sim 2\left(\frac{\dot{\gamma}}{2\kappa}\right)^{2/3}\mathrm{We}^{-(m-1)/3}, \quad T_{12} \sim \left(\frac{\dot{\gamma}}{2\kappa}\right)^{1/3}\mathrm{We}^{-(m+2)/6} \qquad \text{as We} \to \infty. \tag{2.10}$$

Thus the influence of the linear stress terms in (2.5)–(2.7) are negligible. We conclude that if a general boundary layer is to recover viscometric behaviour then we are required to balance the upper convective stress derivative, quadratic stress and rate of strain terms in the constitutive equations.

(b) For $\kappa = o(1)$ the behaviour (2.10) will hold until $\kappa = O(\mathrm{We}^{-(4-m)})$ at which point the linear stress terms now enter the dominant balance. Setting $\kappa = \hat{\kappa}\mathrm{We}^{-(4-m)}$ with $\hat{\kappa} = O(1)$ we obtain

$$T_{11} \sim a_{11}\mathrm{We}^{3-m}, \quad T_{12} \sim a_{12}\mathrm{We}^{-\frac{(m-2)}{2}} \qquad \text{as We} \to \infty, \tag{2.11}$$

where $a_{11} = 2a_{12}^2$ with $a_{12}$ and $a_{11}$ satisfying

$$a_{12} + 2\hat{\kappa}a_{12}^3 = \dot{\gamma}, \qquad a_{11}(1+\hat{\kappa}a_{11})^2 = 2\dot{\gamma}^2. \tag{2.12}$$

Here then, the linear stress terms enter the balance with the upper convective stress derivative, quadratic stress and rate of strain terms in the constitutive equations.

(c) For $\kappa = o(\mathrm{We}^{-(4-m)})$ then we again obtain (2.11) but now with $a_{12} = \dot{\gamma}$ and $a_{11} = 2\dot{\gamma}^2$. These follow from the results in (b) for $\hat{\kappa} = o(1)$. Now viscometric behaviour is that obtained for the UCM model and given by the balance between the linear stress terms, upper convective stress derivative and rate of strain terms. The quadratic stress terms being negligible.

Thus we have the important conclusion that there are three distinct wall viscometric behaviours for the PTT model, that occur according to the size of the PTT model parameter $\kappa$. We may summarize these behaviours by noting that they are given by balances between components in the following groups of terms in the constitutive equations

$$\left\{\overset{\triangledown}{\mathbf{T}}, (\mathrm{tr}\mathbf{T})\mathbf{T}, 2\mathbf{D}\right\}, \qquad \left\{\mathbf{T}, \overset{\triangledown}{\mathbf{T}}, (\mathrm{tr}\mathbf{T})\mathbf{T}, 2\mathbf{D}\right\}, \qquad \left\{\mathbf{T}, \overset{\triangledown}{\mathbf{T}}, 2\mathbf{D}\right\}, \tag{2.13}$$

each occuring according to the size of $\kappa$ (relative to We). Any boundary layer equations that are derived, must reflect one of these three distinct balances.

The analysis of [3] considered the specific case $m = 2$, with the shear rate maintained at $O(1)$ in the high Weissenberg limit. From (2.10) and (2.11) we have

$$T_{11} = O(\mathrm{We}^{-1/3}), \quad T_{12} = O(\mathrm{We}^{-2/3}), \qquad \text{for } \kappa = O(1)$$

and

$$T_{11} = O(\mathrm{We}), \quad T_{12} = O(1), \qquad \text{for } \kappa = O(\mathrm{We}^{-2}),$$

which are the scalings adopted in [3] for these extra-stress components within the single boundary layer structures that were considered in that article.

When considering separable limiting behaviour for the stream function and extra-stresses from the core, the other case of relevance is when $T_{11} = O(1)$. It then follows from (2.10) and (2.11) that the critical exponents are $m = 1$ for $\kappa = O(1)$ flows and $m = 3$ for $\kappa = o(1)$ flows. These two critical exponents play a central role in the structures that we consider below. Rather remarkably, (2.10) and (2.11) then retrieve the Weissenberg scalings for the extra-stresses $T_{11}$ and $T_{12}$ that we will obtain later for the single boundary layer structures. As such and with regard to this structure only, we could replace $m$ with $n$, the main exponent in the paper which is introduced in the next section.

## 3. The $\kappa = O(1)$ flows

At leading order in the outer region, (1.2) gives

$$\overset{\triangledown}{\mathbf{T}} + \kappa(\mathrm{tr}\mathbf{T})\mathbf{T} = 0 \qquad \text{as We} \to \infty. \tag{3.1}$$

The general solution to (3.1) with (1.1) has been discussed briefly in section 5 of [7], where it is argued that this balance is in fact of limited application and it is the balance (4.2) of the next section that is expected to be most prominent. Nevertheless, it is instructive to consider this case, if only to place the results of the next section in context.

We assume a flat boundary (which can be relaxed as discussed in [6]) and adopt Cartesian axes $(x, y)$ orientated with $x$ along the boundary and $y$ along its normal into the flow domain $y > 0$. As the boundary is approached, we make the assumption that the stream function has the leading order limiting behaviour

$$\psi \sim c_0(x)y^n \qquad \text{as } y \to 0, \tag{3.2}$$

for some arbitrary function $c_0(x)$ and power $n$. Such a separable form for the stream function, would arise if the solution in the core is self-similar or has limiting self-similar behaviour. Whilst this algebraic behaviour in $y$ is not the most general form for the stream function that tends to zero at the solid boundary, it does allow for a systematic classification of boundary layer structures. We also consider extra-stresses with separable behaviour of the form

$$T_{11} \sim c_{11}(x)y^{n-1}, \quad T_{12} \sim c_{12}(x)y^{n}, \quad T_{22} \sim c_{22}(x)y^{n+1} \qquad \text{as } y \to 0, \tag{3.3}$$

where the indices $_1$ and $_2$ are associated with the $x$ and $y$ directions respectively. Explicit expressions for the $c_{ij}(x)$ in terms of $c_0(x)$ are derived in appendix A, where this choice for the exponents of $y$ in these expressions are also explained. The component form of the momentum equations then give

$$\mathrm{Re} n c_0(x)c_0'(x)y^{2(n-1)} = -\frac{\partial p}{\partial x} + y^{n-1}\left(c_{11}'(x) + nc_{12}(x) + o(1)\right), \tag{3.4}$$

$$\mathrm{Re} n(c_0'(x)^2 - c_0(x)c_0''(x))y^{(2n-1)} = -\frac{\partial p}{\partial y} + y^{n}\left(c_{12}'(x) + (n+1)c_{22}(x) + o(1)\right), \tag{3.5}$$

in the limit $y \to 0$. Here $'$ denotes $d/dx$. Thus for $n = 1$, the pressure gradient is retained at leading order and we have $p = p(x)$ where

$$p'(x) = c_{11}'(x) + c_{12}(x) - \mathrm{Re} c_0(x)c_0'(x). \tag{3.6}$$

The inertia terms enter this expression and are negligible only for creeping flows $\mathrm{Re} \ll 1$. When $n > 1$, the inertia terms are now negligible at leading order and we have

$$p = p_0 + O(y^{n+1}), \qquad c_{12}(x) = -\frac{c_{11}'(x)}{n}, \tag{3.7}$$

where $p_0$ is a constant.

The outer solution (3.2) and (3.3) does not give viscometric behaviour at the wall consistent with case (a) in section 2 due to the omission of the rate of strain terms in the approximation of (3.1) to (1.2). We now consider an inner region in which such terms are recovered at leading order.

The limiting behaviours (3.2) and (3.3), suggest considering inner variables given by the scalings

$$x = X, \quad y = \delta Y, \quad \psi = \delta^n \Psi, \quad p = \bar{p}, \quad T_{11} = \delta^{n-1}\bar{T}_{11}, \quad T_{12} = \delta^{n}\bar{T}_{12}, \quad T_{22} = \delta^{n+1}\bar{T}_{22}. \tag{3.8}$$

The gauge $\delta = \delta(\mathrm{We})$ is assumed small and is to be determined by balancing terms in the constitutive equations. The component form of (1.1)–(1.2) gives for the inner region $X = O(1), Y = O(1)$ the equations

$$\delta^{2(n-1)}\mathrm{Re}\left(\frac{\partial \Psi}{\partial Y}\frac{\partial^2 \Psi}{\partial X \partial Y} - \frac{\partial \Psi}{\partial X}\frac{\partial^2 \Psi}{\partial Y^2}\right) = -\frac{\partial \bar{p}}{\partial X} + \delta^{n-1}\left(\frac{\partial \bar{T}_{11}}{\partial X} + \frac{\partial \bar{T}_{12}}{\partial Y}\right), \tag{3.9}$$

$$\delta^{2n}\mathrm{Re}\left(-\frac{\partial \Psi}{\partial Y}\frac{\partial^2 \Psi}{\partial X^2} + \frac{\partial \Psi}{\partial X}\frac{\partial^2 \Psi}{\partial Y \partial X}\right) = -\frac{\partial \bar{p}}{\partial Y} + \delta^{n+1}\left(\frac{\partial \bar{T}_{12}}{\partial X} + \frac{\partial \bar{T}_{22}}{\partial Y}\right), \tag{3.10}$$

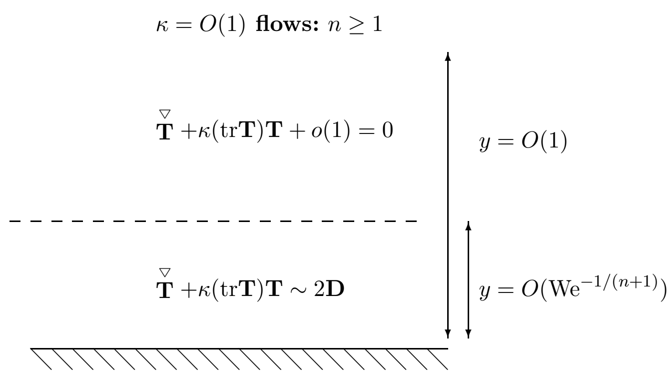


Figure 1: Illustration of the PTT high Weissenberg number boundary layers for the $\kappa = O(1)$ flows. We assume that the core stream function has the solid boundary behaviour (3.2), which introduces a parameter $n$ that may be used to distinguish the structures. The range $n \geq 1$ is considered in this paper. The case $n = 1$ retains the pressure gradient at leading order within the boundary layer and for which the inertia terms in the momentum equation are no longer negligible unless $\mathrm{Re} \ll 1$. In the case $n > 1$ the pressure gradient is now no longer present at leading order within the boundary layer equations, and the inertia terms are uniformly negligible even when $\mathrm{Re} = O(1)$. The case $n = 1$ is expected to be the most important since the loss of the pressure gradient for $n > 1$ appears to severely restrict admissible limiting core behaviours.

and for the constitutive relations

$$\delta^2\bar{T}_{11}+\delta^{(n+1)}\mathrm{We}\left(\frac{\partial\Psi}{\partial Y}\frac{\partial\bar{T}_{11}}{\partial X}-\frac{\partial\Psi}{\partial X}\frac{\partial\bar{T}_{11}}{\partial Y}-2\frac{\partial^2\Psi}{\partial Y^2}\bar{T}_{12}-2\frac{\partial^2\Psi}{\partial X\partial Y}\bar{T}_{11}\right.$$
$$\left.+\kappa\bar{T}_{11}\left(\bar{T}_{11}+\delta^2\bar{T}_{22}\right)\right)=2\delta^2\frac{\partial^2\Psi}{\partial X\partial Y},\tag{3.11}$$
$$\delta^2\bar{T}_{22}+\delta^{(n+1)}\mathrm{We}\left(\frac{\partial\Psi}{\partial Y}\frac{\partial\bar{T}_{22}}{\partial X}-\frac{\partial\Psi}{\partial X}\frac{\partial\bar{T}_{22}}{\partial Y}+2\frac{\partial^2\Psi}{\partial X^2}\bar{T}_{12}+2\frac{\partial^2\Psi}{\partial X\partial Y}\bar{T}_{22}\right.$$
$$\left.+\kappa\bar{T}_{22}\left(\bar{T}_{11}+\delta^2\bar{T}_{22}\right)\right)=-2\frac{\partial^2\Psi}{\partial X\partial Y},\tag{3.12}$$
$$\delta^2\bar{T}_{12}+\delta^{(n+1)}\mathrm{We}\left(\frac{\partial\Psi}{\partial Y}\frac{\partial\bar{T}_{12}}{\partial X}-\frac{\partial\Psi}{\partial X}\frac{\partial\bar{T}_{12}}{\partial Y}+\frac{\partial^2\Psi}{\partial X^2}\bar{T}_{11}-\frac{\partial^2\Psi}{\partial Y^2}\bar{T}_{22}\right.$$
$$\left.+\kappa\bar{T}_{12}\left(\bar{T}_{11}+\delta^2\bar{T}_{22}\right)\right)=\left(\frac{\partial^2\Psi}{\partial Y^2}-\delta^2\frac{\partial^2\Psi}{\partial X^2}\right).\tag{3.13}$$

Matching to the outer solution (3.2)–(3.3) requires

$$\text{as } Y\to\infty\quad \Psi\sim c_0(X)Y^n,\ \ \bar{T}_{11}\sim c_{11}(X)Y^{n-1},\ \ \bar{T}_{12}\sim c_{12}(X)Y^n,\ \ \bar{T}_{22}\sim c_{22}(X)Y^{n+1}.\tag{3.14}$$

The solid boundary and no slip conditions at the wall require

$$\text{at}\quad Y=0,\quad \Psi=\frac{\partial\Psi}{\partial Y}=0.\tag{3.15}$$

The fullest balance in (3.11)–(3.13) occurs when $\delta=\mathrm{We}^{-1/(n+1)}$ which gives the leading order boundary layer equations stated in [3]. The momentum equations (3.9)–(3.10) indicate that the cases $n=1$ and $n>1$ need to be distinguished, which correspond to the pressure gradient being retained at leading order or entering at higher order, respectively. Figure 1 summarises the two structures we are about to consider.

### 3.1 The $n=1$ structure

In this case $\delta=\mathrm{We}^{-1/2}$ and we obtain the leading order boundary layer equations in $X=O(1), Y=O(1)$ as

$$\mathrm{Re}\left(\frac{\partial\Psi}{\partial Y}\frac{\partial^2\Psi}{\partial X\partial Y}-\frac{\partial\Psi}{\partial X}\frac{\partial^2\Psi}{\partial Y^2}\right)=-\frac{d\bar{p}}{dX}+\frac{\partial\bar{T}_{11}}{\partial X}+\frac{\partial\bar{T}_{12}}{\partial Y},\tag{3.16}$$
$$\left(\frac{\partial\Psi}{\partial Y}\frac{\partial\bar{T}_{11}}{\partial X}-\frac{\partial\Psi}{\partial X}\frac{\partial\bar{T}_{11}}{\partial Y}-2\frac{\partial^2\Psi}{\partial Y^2}\bar{T}_{12}-2\frac{\partial^2\Psi}{\partial X\partial Y}\bar{T}_{11}+\kappa\bar{T}_{11}^2\right)=0,\tag{3.17}$$
$$\left(\frac{\partial\Psi}{\partial Y}\frac{\partial\bar{T}_{22}}{\partial X}-\frac{\partial\Psi}{\partial X}\frac{\partial\bar{T}_{22}}{\partial Y}+2\frac{\partial^2\Psi}{\partial X^2}\bar{T}_{12}+2\frac{\partial^2\Psi}{\partial X\partial Y}\bar{T}_{22}+\kappa\bar{T}_{11}\bar{T}_{22}\right)=-2\frac{\partial^2\Psi}{\partial X\partial Y},\tag{3.18}$$
$$\left(\frac{\partial\Psi}{\partial Y}\frac{\partial\bar{T}_{12}}{\partial X}-\frac{\partial\Psi}{\partial X}\frac{\partial\bar{T}_{12}}{\partial Y}+\frac{\partial^2\Psi}{\partial X^2}\bar{T}_{11}-\frac{\partial^2\Psi}{\partial Y^2}\bar{T}_{22}+\kappa\bar{T}_{11}\bar{T}_{12}\right)=\frac{\partial^2\Psi}{\partial Y^2}.\tag{3.19}$$

The equations (3.16)–(3.19) are subject to the matching conditions (3.14) with $n=1$ where (3.6) indicates that the pressure gradient satisfies

$$\bar{p}'(X)=c_{11}'(X)+c_{12}(X)-\mathrm{Re}c_0(X)c_0'(X).\tag{3.20}$$

Expressions for $c_{ij}(X)$ in terms of a general $c_0(X)$ are given in (A.13)–(A.15) in appendix A.1. Considering the wall behaviour of (3.16)–(3.19) we have

$$\text{as } Y \to 0 \qquad \begin{aligned} \Psi &= \kappa a(X)^3 Y^2 + \kappa a(X)^4 b(X) Y^3 + O(Y^4), \\ \bar{T}_{11} &= 2a(X)^2 + 2a(X)^2(2a(X)b(X) - a'(X))Y + O(Y^2), \\ \bar{T}_{12} &= a(X) + a(X)(a(X)b(X) - 6a'(X))Y + O(Y^2), \\ \bar{T}_{22} &= -6a'(X)Y + O(Y^2), \end{aligned} \tag{3.21}$$

with

$$\bar{p}'(X) = a(X)\left(a(X)b(X) - 2a'(X)\right), \tag{3.22}$$

which recovers appropriate viscometric behaviour. We note that this wall behaviour contains two freely specifiable functions $a(X)$ and $b(X)$, which through (3.22) and (3.20) are linked to the outer stress behaviour. The asymptotic behaviour (3.21) covers both the analytic and non-analytic cases for the wall expansion. As in the UCM case, the former arises when $a(X) < 0$ and the latter when $a(X) > 0$ (with now the presence of exponentially small terms). The details will be recorded elsewhere.

In general, we anticipate that these wall and matching behaviours allow for the suitable specification of well-posed boundary value problems. The natural stress basis is a common formulation which gives significant decoupling between the equations and for completeness is given for these boundary layer equations in appendix B.

### 3.2 The $n > 1$ structures

When $n > 1$, a non-trivial balance in (3.11)–(3.13) occurs for $\delta = \mathrm{We}^{-1/(n+1)}$, to give the leading order boundary layer equations in $X = O(1), Y = O(1)$ as again (3.17)–(3.19). However, in place of (3.16) we have

$$0 = \frac{\partial \bar{T}_{11}}{\partial X} + \frac{\partial \bar{T}_{12}}{\partial Y}, \tag{3.23}$$

the pressure gradient no longer entering at leading order. These equations are subject to the matching conditions (3.14). However, the loss of the pressure gradient now places a constraint on $c_{11}$ and $c_{12}$ as given by (3.7). Explicit expressions for the $c_{ij}$ are given in appendix A.2. However, we note that these only contain one arbitrary constant and the loss of the pressure gradient gives rise to the equation (A.27). This equation may be thought of as a constraint on admissible functions $c_0$ and exponents $n$ and severely restricts the general applicability of this structure. For example, this structure cannot capture behaviours in which $c_0$ is an algebraic power of $x$ and furthermore, when $c_0$ is a constant then only $n = 2$ is permissible.

For wall behaviour we now have

$$\text{as } Y \to 0 \qquad \begin{aligned} \Psi &= \kappa a(X)^3 Y^2 + 2\kappa a(X)^3 a'(X) Y^3 + O(Y^4), \\ \bar{T}_{11} &= 2a(X)^2 + 6a(X)^2 a'(X)Y + O(Y^2), \\ \bar{T}_{12} &= a(X) - 4a(X)a'(X)Y + O(Y^2), \\ \bar{T}_{22} &= -6a'(X)Y + O(Y^2), \end{aligned} \tag{3.24}$$

which has the appropriate viscometric behaviour. This behaviour can be obtained from (3.21) by setting $b(X) = 2a'(X)/a(X)$ and consequently only contains one freely specifiable function $a(X)$.

## 4. The $\kappa = o(1)$ flows

We now consider the other core balance of relevance which arises for $\kappa = o(1)$. By this we mean that we are considering now the simultaneous double limit $\kappa \to 0$ and $\mathrm{We} \to \infty$. Consequently, we may consider our problem as having two small independent parameters $\kappa$ and $\mathrm{We}^{-1}$. To systematically describe the distinguished limits that arise, we write $\kappa$ as follows

$$\kappa = \frac{\hat{\kappa}}{\mathrm{We}^r} \tag{4.1}$$

and consider $r > 0$ with $\hat{\kappa} = O(1)$. Our goal here will be to determine the boundary layer structures associated with different ranges of $r$ and the exponent $n$ (which again is introduced in the limiting behaviour of the core stream function through (4.3) below). The resulting equations will involve the parameter $\hat{\kappa}$ (sometimes termed a similarity parameter, see Kevorkian and Cole [4]) which represents the ratio $\kappa/\mathrm{We}^{-r}$ of a combination of the two small independent parameters $\kappa$ and $\mathrm{We}^{-1}$. This is a far more convenient way to categorise the possible dominant balances for relative sizes of the two small independent parameters, when compared to considering expansions involving the simultaneous double limits $\kappa \to 0$ and $\mathrm{We}^{-1} \to 0$. We emphasize that $r > 0$ can take any positive value and is fixed for any given situation, its value quantifying the size of $\kappa$ relative to $\mathrm{We}^{-1}$.

At leading order in the outer region, (1.2) now gives

$$\overset{\triangledown}{\mathbf{T}} = 0 \qquad \text{as We} \to \infty. \tag{4.2}$$

As the boundary is approached, we again consider separable behaviour for the stream function and extra-stresses in the form

$$\psi \sim c_0(x)y^n, \quad T_{11} \sim c_{11}(x), \quad T_{12} \sim c_{12}(x)y, \quad T_{22} \sim c_{22}(x)y^2 \qquad \text{as } y \to 0, \tag{4.3}$$

for some arbitrary function $c_0(x)$ and power $n$. Explicit expressions for the $c_{ij}(x)$ in terms of $c_0(x)$ have been derived in [1]. The component form of the momentum equations then give

$$\mathrm{Re}nc_0(x)c_0'(x)y^{2(n-1)} = -\frac{\partial p}{\partial x} + c_{11}'(x) + c_{12}(x) + o(1), \tag{4.4}$$

$$\mathrm{Re}n(c_0'(x)^2 - c_0(x)c_0''(x))y^{(2n-1)} = -\frac{\partial p}{\partial y} + y\left(c_{12}'(x) + 2c_{22}(x)\right) + o(y), \tag{4.5}$$

in the limit $y \to 0$. For $n \geq 1$, the pressure gradient is retained at leading order and we have $p = p(x)$ where

$$p'(x) = c_{11}'(x) + c_{12}(x) - \mathrm{Re}c_0(x)c_0'(x)\delta_{n1}. \tag{4.6}$$

Here we have introduced a Kronecker delta to combine the $n = 1$ and $n > 1$ cases together. If $n = 1$ then the inertia terms are retained at leading order if $\mathrm{Re} = O(1)$ and are negligible only for creeping flows $\mathrm{Re} \ll 1$. If $n > 1$ then they are uniformly negligible even when $\mathrm{Re} = O(1)$.

We now address the recovery of the linear stress, quadratic stress and rate-of-strain terms as appropriate in the constitutive equations. The limiting behaviours (4.3) suggest considering inner variables given by the scalings

$$x = X, \quad y = \delta Y, \quad \psi = \delta^n \Psi, \quad p = \bar{p}, \quad T_{11} = \bar{T}_{11}, \quad T_{12} = \delta \bar{T}_{12}, \quad T_{22} = \delta^2 \bar{T}_{22}, \tag{4.7}$$

with the gauge $\delta = \delta(\mathrm{We})$ as usual to be determined. The component form of (1.1)–(1.2) gives for the inner region $X = O(1), Y = O(1)$ the equations

$$\delta^{2(n-1)}\mathrm{Re}\left(\frac{\partial\Psi}{\partial Y}\frac{\partial^2\Psi}{\partial X\partial Y} - \frac{\partial\Psi}{\partial X}\frac{\partial^2\Psi}{\partial Y^2}\right) = -\frac{\partial\bar{p}}{\partial X} + \left(\frac{\partial\bar{T}_{11}}{\partial X} + \frac{\partial\bar{T}_{12}}{\partial Y}\right), \tag{4.8}$$

$$\delta^{2n}\mathrm{Re}\left(-\frac{\partial\Psi}{\partial Y}\frac{\partial^2\Psi}{\partial X^2} + \frac{\partial\Psi}{\partial X}\frac{\partial^2\Psi}{\partial Y\partial X}\right) = -\frac{\partial\bar{p}}{\partial Y} + \delta^2\left(\frac{\partial\bar{T}_{12}}{\partial X} + \frac{\partial\bar{T}_{22}}{\partial Y}\right), \tag{4.9}$$

and for the constitutive relations

$$\bar{T}_{11} + \delta^{(n-1)}\mathrm{We}\left(\frac{\partial\Psi}{\partial Y}\frac{\partial\bar{T}_{11}}{\partial X} - \frac{\partial\Psi}{\partial X}\frac{\partial\bar{T}_{11}}{\partial Y} - 2\frac{\partial^2\Psi}{\partial Y^2}\bar{T}_{12} - 2\frac{\partial^2\Psi}{\partial X\partial Y}\bar{T}_{11}\right) + \hat{\kappa}\mathrm{We}^{1-r}\bar{T}_{11}\left(\bar{T}_{11} + \delta^2\bar{T}_{22}\right) = 2\delta^{n-1}\frac{\partial^2\Psi}{\partial X\partial Y}, \tag{4.10}$$

$$\bar{T}_{22} + \delta^{(n-1)}\mathrm{We}\left(\frac{\partial\Psi}{\partial Y}\frac{\partial\bar{T}_{22}}{\partial X} - \frac{\partial\Psi}{\partial X}\frac{\partial\bar{T}_{22}}{\partial Y} + 2\frac{\partial^2\Psi}{\partial X^2}\bar{T}_{12} + 2\frac{\partial^2\Psi}{\partial X\partial Y}\bar{T}_{22}\right) + \hat{\kappa}\mathrm{We}^{1-r}\bar{T}_{22}\left(\bar{T}_{11} + \delta^2\bar{T}_{22}\right) = -2\delta^{n-3}\frac{\partial^2\Psi}{\partial X\partial Y}, \tag{4.11}$$

$$\bar{T}_{12} + \delta^{(n-1)}\mathrm{We}\left(\frac{\partial\Psi}{\partial Y}\frac{\partial\bar{T}_{12}}{\partial X} - \frac{\partial\Psi}{\partial X}\frac{\partial\bar{T}_{12}}{\partial Y} + \frac{\partial^2\Psi}{\partial X^2}\bar{T}_{11} - \frac{\partial^2\Psi}{\partial Y^2}\bar{T}_{22}\right) + \hat{\kappa}\mathrm{We}^{1-r}\bar{T}_{12}\left(\bar{T}_{11} + \delta^2\bar{T}_{22}\right) = \delta^{n-3}\left(\frac{\partial^2\Psi}{\partial Y^2} - \delta^2\frac{\partial^2\Psi}{\partial X^2}\right). \tag{4.12}$$

Matching to the outer solution (4.3) and (4.6) requires

$$\text{as } Y \to \infty \quad \Psi \sim c_0(X)Y^n, \;\; \bar{T}_{11} \sim c_{11}(X), \;\; \bar{T}_{12} \sim c_{12}(X)Y, \;\; \bar{T}_{22} \sim c_{22}(X)Y^2, \tag{4.13}$$

with

$$\bar{p}'(X) = c_{11}'(X) + c_{12}(X) - \mathrm{Re}c_0(X)c_0'(X)\delta_{n1}. \tag{4.14}$$

The solid boundary and no slip conditions at the wall require

$$\text{at} \quad Y = 0, \quad \Psi = \frac{\partial\Psi}{\partial Y} = 0. \tag{4.15}$$

To derive the boundary layer equations, we now determine systematically the possible dominant balances in (4.10)–(4.12). There are in fact nine distinct non-trivial balances between the respective terms, which will be described below. However, we begin by considering the situation for small $r$. The linear stress terms are then uniformly subdominant and there are three possible balances. The fullest is where the upper convective derivative terms balance the quadratic stress and rate of strain terms which gives rise to a single layer structure. The other possible balances are that of the upper convective derivative with either the quadratic stress terms or the rate of strain terms only, each giving rise to double layer structure where the omitted terms are retrieved in additional regions near to the boundary. Then, as $r$ increases, the possibility occurs of the linear stress terms now entering the leading order equations for these structures and gives rise to an additional three dominant balances (one for each of the aforementioned structures). As $r$ increases further, then the quadratic stress terms become negligible and are lost at leading order, retrieving the UCM boundary layer equations, again of which there are three.

Since two distinct types of double layer structures arise, we will distinguish them by giving the labels of type I and II. A type I structure occurs if there is a balance between the upper convective stress derivative and either the linear or quadratic stress terms within the main part (i.e. the inner region) of the boundary layer. A type II structure occurs if the balance in the main part of the boundary layer is between the upper convective stress derivative and the rate of strain terms.

Each of the nine structures described below is distinct and to avoid proliferation of notation we shall use bars to denote inner variables and hats to denote inner inner variables. This will be the case when considering different values of $r$ for the single region as well as the type I and II structures. Bearing this in mind, then no confusion should arise through duplication of notation. We do not comment here on the relative importance of these structures, but simply give the expected boundary layer structure and equations for given $n > 1$ and $r > 0$ which are summarized later in Figure 5. Comments regarding the value of $n$ for these structures are made in the discussion section. Arguably the single layer structure should for now receive the greatest attention, followed by the type I double layer structure.

### 4.1 The single layer structure

Seeking the fullest balance in (4.10)–(4.12), we need to consider separately the cases $0 < r < 1$, $r = 1$ and $r > 1$. For a given value of $r$, we will find that there is a unique value of $n$ namely $n = 1 + 2r$ for $0 < r < 1$ and $n = 3$ for $r \geq 1$. The three structures that we are about to describe are summarised in Figure 2 and represent the three balances given in (2.13) identified for viscometric behaviour at the wall.

#### 4.1.1 The range $0 < r < 1$

To balance the upper convected derivative, quadratic stress and rate of strain terms in (4.10)–(4.12), we require

$$n = 1 + 2r \qquad \text{and} \qquad \delta = \mathrm{We}^{-1/2}.$$

This gives the leading order boundary layer equations in $X = O(1), Y = O(1)$ as

$$0 = -\frac{d\bar{p}}{dX} + \frac{\partial \bar{T}_{11}}{\partial X} + \frac{\partial \bar{T}_{12}}{\partial Y}, \tag{4.16}$$

$$\left(\frac{\partial \Psi}{\partial Y}\frac{\partial \bar{T}_{11}}{\partial X} - \frac{\partial \Psi}{\partial X}\frac{\partial \bar{T}_{11}}{\partial Y} - 2\frac{\partial^2 \Psi}{\partial Y^2}\bar{T}_{12} - 2\frac{\partial^2 \Psi}{\partial X \partial Y}\bar{T}_{11}\right) + \hat{\kappa}\bar{T}_{11}^2 = 0, \tag{4.17}$$

$$\left(\frac{\partial \Psi}{\partial Y}\frac{\partial \bar{T}_{22}}{\partial X} - \frac{\partial \Psi}{\partial X}\frac{\partial \bar{T}_{22}}{\partial Y} + 2\frac{\partial^2 \Psi}{\partial X^2}\bar{T}_{12} + 2\frac{\partial^2 \Psi}{\partial X \partial Y}\bar{T}_{22}\right) + \hat{\kappa}\bar{T}_{11}\bar{T}_{22} = -2\frac{\partial^2 \Psi}{\partial X \partial Y}, \tag{4.18}$$

$$\left(\frac{\partial \Psi}{\partial Y}\frac{\partial \bar{T}_{12}}{\partial X} - \frac{\partial \Psi}{\partial X}\frac{\partial \bar{T}_{12}}{\partial Y} + \frac{\partial^2 \Psi}{\partial X^2}\bar{T}_{11} - \frac{\partial^2 \Psi}{\partial Y^2}\bar{T}_{22}\right) + \hat{\kappa}\bar{T}_{11}\bar{T}_{12} = \frac{\partial^2 \Psi}{\partial Y^2}. \tag{4.19}$$

These are the boundary layer equations (3.16)–(3.19) obtained in the $n = 1, \kappa = O(1)$ case (with $\mathrm{Re} = o(1)$) in section 3.1, this case being recovered by taking the limit $r \to 0$. The equations (3.16)–(3.19) are subject to the matching conditions (4.13) with $n = 1 + 2r$ and the pressure gradient satisfying (4.14) (Kronecker delta being zero for $r > 0$). At the wall we have the viscometric behaviour (3.21) with (3.22) and now $\kappa$ replaced with $\hat{\kappa}$.

It may be verified that the omitted linear stress terms have magnitude $O(\delta^{2(1-r)}) = O(\mathrm{We}^{-(1-r)})$. This suggests that these terms are first recovered at the critical exponent $r = r_1 = 1$, which we consider next.

#### 4.1.2 The case $r = r_1 = 1$

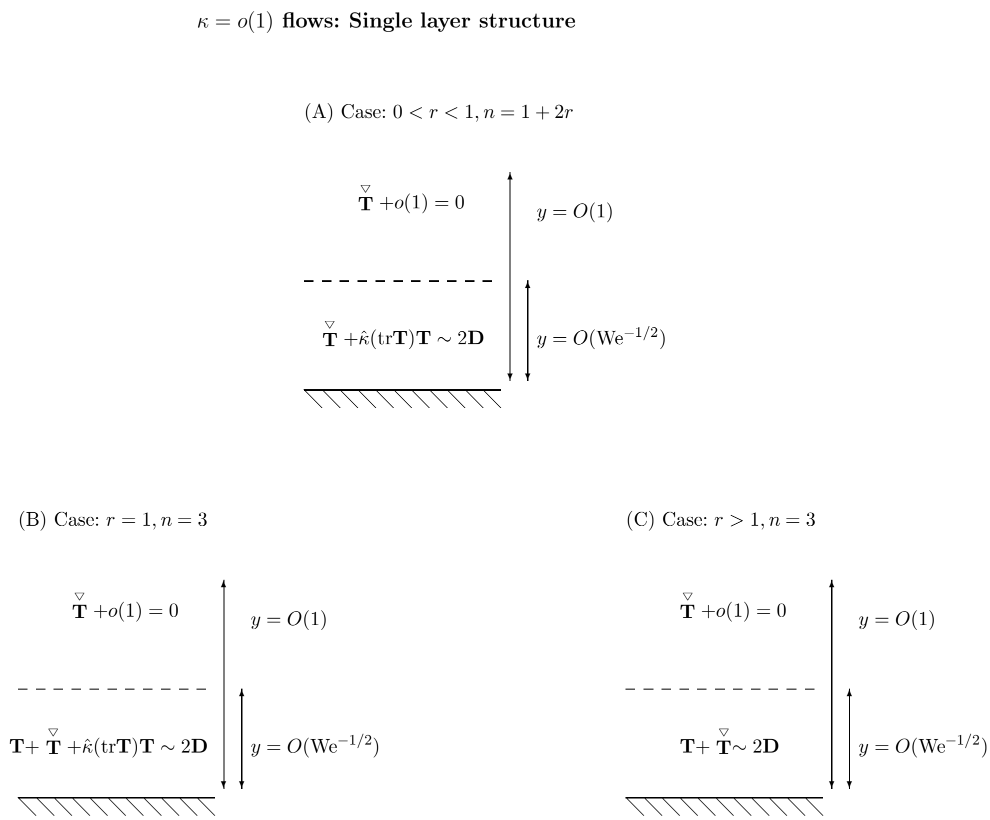


Figure 2: High Weissenberg number boundary layers in $\kappa = o(1)$ flows. Shown are the single layer structures that arise for different sizes of the model parameter $\kappa = \hat{\kappa}\mathrm{We}^{-r}$. These structures occur for different values of $r > 0$ and the exponent $n$ is introduced through the limiting behaviour (4.3) of the stream function from the core. (A) shows the case $0 < r < 1$ with $n$ determined uniquely as $n = 1 + 2r$. The shown balance holds until $r = 1$ in which case (B) occurs where the linear stress terms now enter the boundary layer equations at leading order. For $r > 1$ the quadratic stress terms are now subdominant and we obtain at leading order the UCM single layer structure shown in (C). In all cases, the boundary layer is of width of $O\left(\mathrm{We}^{-\frac{1}{2}}\right)$.

The fullest balance in (4.10)–(4.12) now gives

$$n = 3, \qquad \delta = \mathrm{We}^{-1/2} \tag{4.20}$$

and we obtain the leading order boundary layer equations in $X = O(1), Y = O(1)$ as

$$0 = -\frac{d\bar{p}}{dX} + \frac{\partial \bar{T}_{11}}{\partial X} + \frac{\partial \bar{T}_{12}}{\partial Y}, \tag{4.21}$$

$$\bar{T}_{11} + \left( \frac{\partial \Psi}{\partial Y}\frac{\partial \bar{T}_{11}}{\partial X} - \frac{\partial \Psi}{\partial X}\frac{\partial \bar{T}_{11}}{\partial Y} - 2\frac{\partial^2 \Psi}{\partial Y^2}\bar{T}_{12} - 2\frac{\partial^2 \Psi}{\partial X \partial Y}\bar{T}_{11} \right) + \hat{\kappa}\bar{T}_{11}^2 = 0, \tag{4.22}$$

$$\bar{T}_{22} + \left( \frac{\partial \Psi}{\partial Y}\frac{\partial \bar{T}_{22}}{\partial X} - \frac{\partial \Psi}{\partial X}\frac{\partial \bar{T}_{22}}{\partial Y} + 2\frac{\partial^2 \Psi}{\partial X^2}\bar{T}_{12} + 2\frac{\partial^2 \Psi}{\partial X \partial Y}\bar{T}_{22} \right) + \hat{\kappa}\bar{T}_{11}\bar{T}_{22} = -2\frac{\partial^2 \Psi}{\partial X \partial Y}, \tag{4.23}$$

$$\bar{T}_{12} + \left( \frac{\partial \Psi}{\partial Y}\frac{\partial \bar{T}_{12}}{\partial X} - \frac{\partial \Psi}{\partial X}\frac{\partial \bar{T}_{12}}{\partial Y} + \frac{\partial^2 \Psi}{\partial X^2}\bar{T}_{11} - \frac{\partial^2 \Psi}{\partial Y^2}\bar{T}_{22} \right) + \hat{\kappa}\bar{T}_{11}\bar{T}_{12} = \frac{\partial^2 \Psi}{\partial Y^2}. \tag{4.24}$$

The equations (4.21)–(4.24) are subject to the matching conditions (4.13) with $n = 3$ where the pressure gradient again satisfies (4.14) (with Kronecker delta being zero). At the wall we now have the viscometric behaviour

$$\begin{aligned}
\Psi &= \frac{1}{2}a(X)Y^2 + \frac{1}{6}b(X)Y^3 + O(Y^4),\\
\bar{T}_{11} &= a_{11}(X) + \left( \frac{2(1+\hat{\kappa}a_{11}(X))a_{11}(X)b(X)}{a(X)(1+3\hat{\kappa}a_{11}(X))} - \frac{6a(X)^2a'(X)}{(1+\hat{\kappa}a_{11}(X))(1+3\hat{\kappa}a_{11}(X))^2} \right) Y + O(Y^2),\\
\bar{T}_{12} &= \frac{a(X)}{(1+\hat{\kappa}a_{11}(X))}\\
&\quad + \left( \frac{b(X)}{(1+3\hat{\kappa}a_{11}(X))} - \frac{2(3+13\hat{\kappa}a_{11}(X)+18\hat{\kappa}^2a_{11}(X)^2)a(X)^3a'(X)}{a_{11}(X)(1+\hat{\kappa}a_{11}(X))^4(1+3\hat{\kappa}a_{11}(X))^2} \right) Y + O(Y^2),\\
\bar{T}_{22} &= -\frac{2a'(X)}{(1+\hat{\kappa}a_{11}(X))}Y + O(Y^2), \qquad \text{as } Y \to 0
\end{aligned} \tag{4.25}$$

with

$$\bar{p}'(X) = \frac{b(X)}{(1+3\hat{\kappa}a_{11}(X))} + \frac{2(1+3\hat{\kappa}a_{11}(X)-6\hat{\kappa}^2a_{11}(X)^2)a(X)^3a'(X)}{a_{11}(X)(1+3\hat{\kappa}a_{11}(X))^2(1+\hat{\kappa}a_{11}(X))^4} \tag{4.26}$$

and $a_{11}(X)$ satisfies

$$a_{11}(X)(1+\hat{\kappa}a_{11}(X))^2 = 2a(X)^2. \tag{4.27}$$

This last equation is the analogue of (2.12) and thus we obtain wall viscometric behaviour consistent with that described in (b) of section 2 and the second balance indicated in (2.13). The analytic part of this wall behaviour contains two freely specifiable functions $a(X)$ and $b(X)$, which through (4.26) and (4.14) are linked to the outer stress behaviour. The coefficients of the higher order terms in the power series expansions again can be expressed in terms of $a(X)$ and $b(X)$ only, the non-analytic part of the expansion (arising in the case $a(X) > 0$) being associated with exponentially small terms. The natural stress basis formulation of these equations in this case are given in appendix B.

**4.1.3 The range $r > 1$**

When $r > 1$, the exponent and scaling as given by (4.20) of the previous subsection persist. Thus we again obtain (4.21)–(4.24), only now with $\hat{\kappa} = o(1)$, so that the quadratic stress terms no longer enter at leading order. The resulting equations are those of the UCM model for the single boundary layer structure as given in [1].

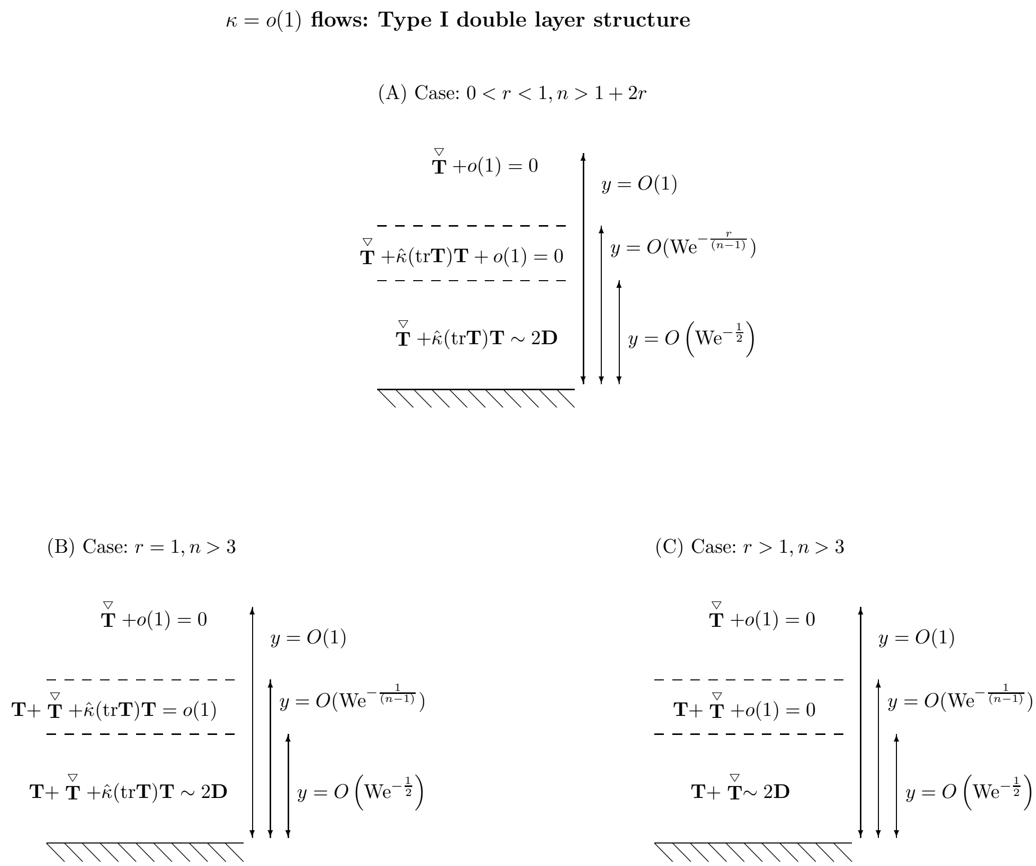


Figure 3: High Weissenberg number boundary layers in $\kappa = o(1)$ flows. Shown are the balances for the type I double boundary layer structures according to the ranges of $r$. The boundary layer is composed of a thick inner region of width that varies with $r$ and $n$ and and an inner inner region of width of $O\left(\mathrm{We}^{-\frac{1}{2}}\right)$ in all cases. (A) shows the case $0 < r < 1$ with $n$ now occuring for the range $n > 1 + 2r$. The shown balance holds until $r = 1$ in which case (B) occurs where the linear stress terms now enter the boundary layer equations at leading order. For $r > 1$ the quadratic stress terms are now subdominant and we obtain at leading order the UCM double layer structure shown in (C).

## 4.2 Type I double layer structure

Here we again distinguish the cases $0 < r < 1, r = 1, r > 1$, as for the single layer structure. In each of these cases, a range of $n$ is permissible namely $n > 1 + 2r$ for $0 < r < 1$ and $n > 3$ for $r \geq 1$. Figure 3 summarises the three type I structures.

### 4.2.1 The range $0 < r < 1$

In addition to the balance of section 4.1.1, a second distinguished limit occurs when

$$n > 1 + 2r \quad \text{and} \quad \delta = \mathrm{We}^{-\frac{r}{(n-1)}}. \tag{4.28}$$

Now the quadratic stress terms balance the upper convected stress derivative with the rate of strain terms subdominant. The leading order boundary layer equations in $X = O(1), Y = O(1)$ are

$$0 = -\frac{d\bar{p}}{dX} + \frac{\partial \bar{T}_{11}}{\partial X} + \frac{\partial \bar{T}_{12}}{\partial Y}, \tag{4.29}$$

$$\left(\frac{\partial \Psi}{\partial Y}\frac{\partial \bar{T}_{11}}{\partial X} - \frac{\partial \Psi}{\partial X}\frac{\partial \bar{T}_{11}}{\partial Y} - 2\frac{\partial^2 \Psi}{\partial Y^2}\bar{T}_{12} - 2\frac{\partial^2 \Psi}{\partial X \partial Y}\bar{T}_{11}\right) + \hat{\kappa}\bar{T}_{11}^2 = 0, \tag{4.30}$$

$$\left(\frac{\partial \Psi}{\partial Y}\frac{\partial \bar{T}_{22}}{\partial X} - \frac{\partial \Psi}{\partial X}\frac{\partial \bar{T}_{22}}{\partial Y} + 2\frac{\partial^2 \Psi}{\partial X^2}\bar{T}_{12} + 2\frac{\partial^2 \Psi}{\partial X \partial Y}\bar{T}_{22}\right) + \hat{\kappa}\bar{T}_{22}\bar{T}_{11} = 0, \tag{4.31}$$

$$\left(\frac{\partial \Psi}{\partial Y}\frac{\partial \bar{T}_{12}}{\partial X} - \frac{\partial \Psi}{\partial X}\frac{\partial \bar{T}_{12}}{\partial Y} + \frac{\partial^2 \Psi}{\partial X^2}\bar{T}_{11} - \frac{\partial^2 \Psi}{\partial Y^2}\bar{T}_{22}\right) + \hat{\kappa}\bar{T}_{12}\bar{T}_{11} = 0. \tag{4.32}$$

In this region the linear stress terms are of size $O(\mathrm{We}^{-(1-r)})$ and the rate of strain terms $O(\mathrm{We}^{\frac{(1+2r-n)}{(n-1)}})$. Matching with outer solution we have (4.13) and (4.14), whilst matching with the inner inner region described below, we are interested in solutions to (4.29)–(4.32) with behaviour

$$\text{as } Y \to 0 \qquad \Psi \sim \bar{c}_0(X)Y, \;\; \bar{T}_{11} \sim \bar{c}_{11}(X), \;\; \bar{T}_{12} \sim \bar{c}_{12}(X)Y, \;\; \bar{T}_{22} \sim \bar{c}_{22}(X)Y^2. \tag{4.33}$$

This limiting behaviour is the case considered in appendix A, and expressions for $\bar{c}_{ij}(X)$ in terms of $\bar{c}_0(X)$ are given by (A.13)–(A.15) allowing for a suitable change of notation ($\bar{c}_{ij}(X)$ and $\bar{c}_0(X)$ in place of $c_{ij}(x)$ and $c_0(x)$ respectively). As particular solutions of (4.29)–(4.32) satisfying (4.13) and (4.33) we have

$$\Psi = \bar{c}_0(X)Y + c_0(X)Y^n, \quad \bar{T}_{11} = c_{11}(X), \quad \bar{T}_{12} = c_{12}(X)Y, \quad \bar{T}_{22} = c_{22}(X)Y^2, \tag{4.34}$$

in the following cases:

$$\begin{aligned} &\text{(a)} \;\; c_0(X) = C_0, \;\; c_{11}(X) = C_1, \;\; c_{12}(X) = 0, \;\; c_{22}(X) = 0, \\ &\qquad \bar{c}_0(X) = \bar{C}_1 + \frac{\kappa}{2}C_0^{\frac{2}{n}}C_1 X, \end{aligned} \tag{4.35}$$

$$\begin{aligned} &\text{(b)} \;\; c_0(X) = C_0 X^{3n-2}, \;\; c_{11}(X) = C_2 X^2, \;\; c_{12}(X) = -3C_2 X, \;\; c_{22}(X) = 9C_2, \\ &\qquad \bar{c}_0(X) = X\left(\bar{C}_1 + \frac{1}{4}\kappa C_2 n X^2\right), \end{aligned} \tag{4.36}$$

$$\begin{aligned} &\text{(c)} \;\; c_0(X) = C_0 X^{-n}, \;\; c_{11}(X) = C_3, \;\; c_{12}(X) = \frac{nC_3}{(n-1)X}, \;\; c_{22}(X) = \frac{(n+1)C_3}{(n-1)X^2}, \\ &\qquad \bar{c}_0(X) = \frac{\kappa C_3}{2}X, \end{aligned} \tag{4.37}$$

where in each case $C_0, C_1, C_2, C_3, \bar{C}_0$ are arbitrary constants and we are interested in $n > 1$. These particular solutions are noteworthy since the far-field stress behaviour recieved by this region from the outer core flow, is maintained througout this region unchanged.

To recover viscometric behaviour at the wall, in the general situation, we consider another region in which the rate of strain terms are retained at leading order. This inner inner region is given by the scalings

$$Y = \theta_1 \hat{Y}, \quad \Psi = \theta_1 \hat{\Psi}, \quad \bar{T}_{11} = \hat{T}_{11}, \quad \bar{T}_{12} = \theta_1 \hat{T}_{12}, \quad \bar{T}_{22} = \theta_1^2 \hat{T}_{22}, \tag{4.38}$$

where $\theta_1 = \delta^{\frac{(n-1-2r)}{2r}} = \mathrm{We}^{-\frac{(n-1-2r)}{2(n-1)}}$. It is noted that $\theta_1 \ll 1$ since $n > 1 + 2r$ and the thickness of this inner inner region is $O(\delta\theta_2) = O(\mathrm{We}^{-\frac{1}{2}})$, i.e. the same as the thickness of the single layer $n = 1 + 2r$ structure. The leading order equations in $X = O(1), \hat{Y} = O(1)$ are now

$$0 = -\frac{d\bar{p}}{dX} + \frac{\partial \hat{T}_{11}}{\partial X} + \frac{\partial \hat{T}_{12}}{\partial \hat{Y}}, \tag{4.39}$$

$$\left(\frac{\partial \hat{\Psi}}{\partial \hat{Y}}\frac{\partial \hat{T}_{11}}{\partial X} - \frac{\partial \hat{\Psi}}{\partial X}\frac{\partial \hat{T}_{11}}{\partial \hat{Y}} - 2\frac{\partial^2 \hat{\Psi}}{\partial \hat{Y}^2}\hat{T}_{12} - 2\frac{\partial^2 \hat{\Psi}}{\partial X \partial \hat{Y}}\hat{T}_{11}\right) + \hat{\kappa}\hat{T}_{11}^2 = 0, \tag{4.40}$$

$$\left(\frac{\partial \hat{\Psi}}{\partial \hat{Y}}\frac{\partial \hat{T}_{22}}{\partial X} - \frac{\partial \hat{\Psi}}{\partial X}\frac{\partial \hat{T}_{22}}{\partial \hat{Y}} + 2\frac{\partial^2 \hat{\Psi}}{\partial X^2}\hat{T}_{12} + 2\frac{\partial^2 \hat{\Psi}}{\partial X \partial \hat{Y}}\hat{T}_{22}\right) + \hat{\kappa}\hat{T}_{22}\hat{T}_{11} = -2\frac{\partial^2 \hat{\Psi}}{\partial X \partial \hat{Y}}, \tag{4.41}$$

$$\left(\frac{\partial \hat{\Psi}}{\partial \hat{Y}}\frac{\partial \hat{T}_{12}}{\partial X} - \frac{\partial \hat{\Psi}}{\partial X}\frac{\partial \hat{T}_{12}}{\partial \hat{Y}} + \frac{\partial^2 \hat{\Psi}}{\partial X^2}\hat{T}_{11} - \frac{\partial^2 \hat{\Psi}}{\partial \hat{Y}^2}\hat{T}_{22}\right) + \hat{\kappa}\hat{T}_{12}\hat{T}_{11} = \frac{\partial^2 \hat{\Psi}}{\partial \hat{Y}^2}, \tag{4.42}$$

with $\bar{p}$ as given in (4.14). At the solid boundary, (3.21) and (3.22) gives the viscometric behaviour (adjusted for current hat variables as appropriate) and matching to the inner solution (4.33) gives the conditions

$$\text{as } \hat{Y} \to \infty \quad \hat{\Psi} \sim \bar{c}_0(X)\hat{Y}, \quad \hat{T}_{11} \sim \bar{c}_{11}(X), \quad \hat{T}_{12} \sim \bar{c}_{12}(X)\hat{Y}, \quad \hat{T}_{22} \sim \bar{c}_{22}(X)\hat{Y}^2. \tag{4.43}$$

The omitted linear stress terms in this region are $O(\delta^{\frac{(n-1)(1-r)}{r}}) = O(\mathrm{We}^{-(1-r)})$, the same size as in the inner region $Y = O(1)$. Such terms will enter the leading order balance when $r = r_1 = 1$.

### 4.2.2 The case $r = r_1 = 1$

The linear stress terms are retrieved in this distinguished limit which occurs for

$$n > 3 \quad \text{and} \quad \delta = \mathrm{We}^{-\frac{1}{(n-1)}}. \tag{4.44}$$

The leading order boundary layer equations in $X = O(1), Y = O(1)$ are now

$$0 = -\frac{d\bar{p}}{dX} + \frac{\partial \bar{T}_{11}}{\partial X} + \frac{\partial \bar{T}_{12}}{\partial Y}, \tag{4.45}$$

$$\bar{T}_{11} + \left(\frac{\partial \Psi}{\partial Y}\frac{\partial \bar{T}_{11}}{\partial X} - \frac{\partial \Psi}{\partial X}\frac{\partial \bar{T}_{11}}{\partial Y} - 2\frac{\partial^2 \Psi}{\partial Y^2}\bar{T}_{12} - 2\frac{\partial^2 \Psi}{\partial X \partial Y}\bar{T}_{11}\right) + \hat{\kappa}\bar{T}_{11}^2 = 0, \tag{4.46}$$

$$\bar{T}_{12} + \left(\frac{\partial \Psi}{\partial Y}\frac{\partial \bar{T}_{22}}{\partial X} - \frac{\partial \Psi}{\partial X}\frac{\partial \bar{T}_{22}}{\partial Y} + 2\frac{\partial^2 \Psi}{\partial X^2}\bar{T}_{12} + 2\frac{\partial^2 \Psi}{\partial X \partial Y}\bar{T}_{22}\right) + \hat{\kappa}\bar{T}_{22}\bar{T}_{11} = 0, \tag{4.47}$$

$$\bar{T}_{22} + \left(\frac{\partial \Psi}{\partial Y}\frac{\partial \bar{T}_{12}}{\partial X} - \frac{\partial \Psi}{\partial X}\frac{\partial \bar{T}_{12}}{\partial Y} + \frac{\partial^2 \Psi}{\partial X^2}\bar{T}_{11} - \frac{\partial^2 \Psi}{\partial Y^2}\bar{T}_{22}\right) + \hat{\kappa}\bar{T}_{12}\bar{T}_{11} = 0. \tag{4.48}$$

Matching to the outer solution we have (4.13) and (4.14), whilst matching with the inner inner region (described below), we again require solutions to (4.45)–(4.48) with limiting behaviour

$$\text{as } Y \to 0 \qquad \Psi \sim \bar{c}_0(X)Y, \;\; \bar{T}_{11} \sim \bar{c}_{11}(X), \;\; \bar{T}_{12} \sim \bar{c}_{12}(X)Y, \;\; \bar{T}_{22} \sim \bar{c}_{22}(X)Y^2. \tag{4.49}$$

In appendix C, the expressions (C.4)–(C.6) give $\bar{c}_{ij}(X)$ in terms of $\bar{c}_0(X)$, with $\bar{p}$ given in (C.8).

In order to recover viscometric behaviour at the wall, we consider another region in which the rate-of-strain terms are retained at leading order. This inner inner region is given by the scalings

$$Y = \theta_1\hat{Y}, \;\; \Psi = \theta_1\hat{\Psi}, \;\; \bar{T}_{11} = \hat{T}_{11}, \;\; \bar{T}_{12} = \theta_1\hat{T}_{12}, \;\; \bar{T}_{22} = \theta_1^2\hat{T}_{22}, \tag{4.50}$$

where $\theta_1 = \delta^{\frac{(n-3)}{2}} = \mathrm{We}^{-\frac{(n-3)}{2(n-1)}}$. It is noted that $\theta_1 \ll 1$ since $n > 3$ and the thickness of this inner inner region is $O(\delta\theta_1) = O(\mathrm{We}^{-\frac{1}{2}})$, i.e. the same as the thickness of the single layer $n = 3$ structure when $r = 1$.

The leading order equations in $X = O(1), \hat{Y} = O(1)$ are now

$$0 = -\frac{d\bar{p}}{dX} + \frac{\partial\hat{T}_{11}}{\partial X} + \frac{\partial\hat{T}_{12}}{\partial\hat{Y}}, \tag{4.51}$$

$$\hat{T}_{11} + \left(\frac{\partial\hat{\Psi}}{\partial\hat{Y}}\frac{\partial\hat{T}_{11}}{\partial X} - \frac{\partial\hat{\Psi}}{\partial X}\frac{\partial\hat{T}_{11}}{\partial\hat{Y}} - 2\frac{\partial^2\hat{\Psi}}{\partial\hat{Y}^2}\hat{T}_{12} - 2\frac{\partial^2\hat{\Psi}}{\partial X\partial\hat{Y}}\hat{T}_{11}\right) + \hat{\kappa}\hat{T}_{11}^2 = 0, \tag{4.52}$$

$$\hat{T}_{22} + \left(\frac{\partial\hat{\Psi}}{\partial\hat{Y}}\frac{\partial\hat{T}_{22}}{\partial X} - \frac{\partial\hat{\Psi}}{\partial X}\frac{\partial\hat{T}_{22}}{\partial\hat{Y}} + 2\frac{\partial^2\hat{\Psi}}{\partial X^2}\hat{T}_{12} + 2\frac{\partial^2\hat{\Psi}}{\partial X\partial\hat{Y}}\hat{T}_{22}\right) + \hat{\kappa}\hat{T}_{22}\hat{T}_{11} = -2\frac{\partial^2\hat{\Psi}}{\partial X\partial\hat{Y}}, \tag{4.53}$$

$$\hat{T}_{12} + \left(\frac{\partial\hat{\Psi}}{\partial\hat{Y}}\frac{\partial\hat{T}_{12}}{\partial X} - \frac{\partial\hat{\Psi}}{\partial X}\frac{\partial\hat{T}_{12}}{\partial\hat{Y}} + \frac{\partial^2\hat{\Psi}}{\partial X^2}\hat{T}_{11} - \frac{\partial^2\hat{\Psi}}{\partial\hat{Y}^2}\hat{T}_{22}\right) + \hat{\kappa}\hat{T}_{12}\hat{T}_{11} = \frac{\partial^2\hat{\Psi}}{\partial\hat{Y}^2}, \tag{4.54}$$

with $\bar{p}$ as given in (C.8). At the solid boundary, (4.25) gives the viscometric behaviour (adjusted for current hat variables as appropriate) and matching to the inner solution (4.49) gives the conditions

$$\text{as } \hat{Y} \to \infty \quad \hat{\Psi} \sim \bar{c}_0(X)\hat{Y}, \;\; \hat{T}_{11} \sim \bar{c}_{11}(X), \;\; \hat{T}_{12} \sim \bar{c}_{12}(X)\hat{Y}, \;\; \hat{T}_{22} \sim \bar{c}_{22}(X)\hat{Y}^2. \tag{4.55}$$

#### 4.2.3 The range $r > 1$

This is a particular case of the previous subsection with $\hat{\kappa} = o(1)$. The scalings (4.44) and (4.50) pertain as do the inner equations (4.45)–(4.48) and inner inner equations (4.51)–(4.54), both with $\hat{\kappa}$ set to zero. These leading order equations are those that occur for the UCM model for the range $n > 3$.

### 4.3 Type II double layer structure

As a third and final structure, we consider cases in which the first terms to be recovered within the boundary layer are the rate of strain terms. This balance will persist with $r$ within the inner region whilst in the inner inner region we recover the quadratic stress terms for $0 < r < r_2$, the linear and quadratic stress terms for $r = r_2$ and the linear stress terms only for $r > r_2$. The critical value $r_2 \geq 1$ is given below in (4.68). Figure 4 summarises the three structures of this type.

#### 4.3.1 The range $0 < r < r_2$

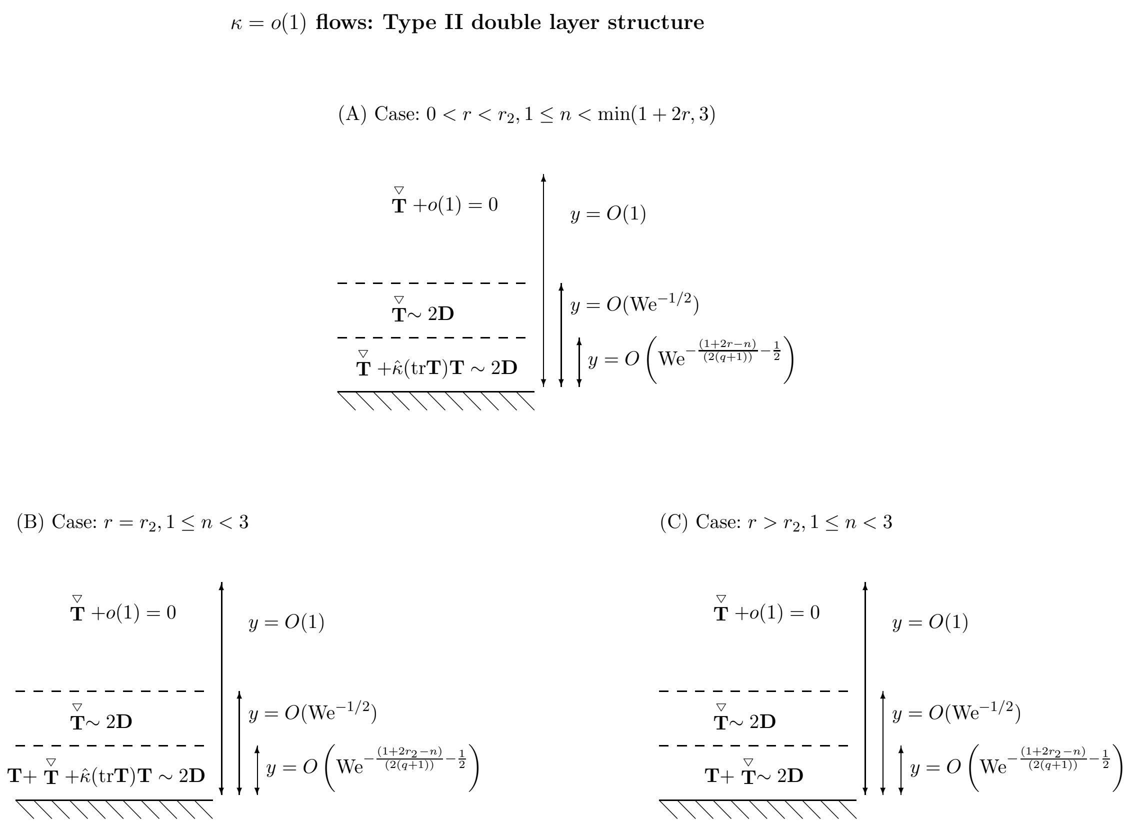


Figure 4: High Weissenberg number boundary layers in $\kappa = o(1)$ flows. Shown are the type II double layer structures composed of the thicker inner region and thinner inner inner region. (A) shows the case $0 < r < r_2$ where $n$ now lies in the range $1 \le n < \min(1 + 2r, 3)$. The shown balance holds until $r = r_2$ which is given later in (4.68). It is noted that $r_2 > 1$. At this point case (B) occurs where the linear stress terms now enter the boundary layer equations at leading order. For $r > r_2$ the quadratic stress terms are now subdominant and we obtain at leading order the UCM single layer structure shown in (C). In all cases, the inner region is of width of $O\left(\mathrm{We}^{-\frac{1}{2}}\right)$.

Complementing the balances of sections 4.1.1 and 4.2.1, a third distinguished limit occurs in (4.10)–(4.12) for

$$1 \leq n < \min(1+2r, 3) \quad \text{and} \quad \delta = \mathrm{We}^{-1/2}. \tag{4.56}$$

Here the range for $n$ allows for the situation in which $r_2 > 1$. The leading order boundary layer equations in the inner region $X = O(1), Y = O(1)$ are now

$$0 = -\frac{d\bar{p}}{dX} + \frac{\partial \bar{T}_{11}}{\partial X} + \frac{\partial \bar{T}_{12}}{\partial Y}, \tag{4.57}$$

$$\left(\frac{\partial \Psi}{\partial Y}\frac{\partial \bar{T}_{11}}{\partial X} - \frac{\partial \Psi}{\partial X}\frac{\partial \bar{T}_{11}}{\partial Y} - 2\frac{\partial^2 \Psi}{\partial Y^2}\bar{T}_{12} - 2\frac{\partial^2 \Psi}{\partial X \partial Y}\bar{T}_{11}\right) = 0, \tag{4.58}$$

$$\left(\frac{\partial \Psi}{\partial Y}\frac{\partial \bar{T}_{22}}{\partial X} - \frac{\partial \Psi}{\partial X}\frac{\partial \bar{T}_{22}}{\partial Y} + 2\frac{\partial^2 \Psi}{\partial X^2}\bar{T}_{12} + 2\frac{\partial^2 \Psi}{\partial X \partial Y}\bar{T}_{22}\right) = -2\frac{\partial^2 \Psi}{\partial X \partial Y}, \tag{4.59}$$

$$\left(\frac{\partial \Psi}{\partial Y}\frac{\partial \bar{T}_{12}}{\partial X} - \frac{\partial \Psi}{\partial X}\frac{\partial \bar{T}_{12}}{\partial Y} + \frac{\partial^2 \Psi}{\partial X^2}\bar{T}_{11} - \frac{\partial^2 \Psi}{\partial Y^2}\bar{T}_{22}\right) = \frac{\partial^2 \Psi}{\partial Y^2}. \tag{4.60}$$

The omitted linear stress terms in this region are of size $O(\delta^{3-n}) = O(\mathrm{We}^{-(3-n)/2})$, whilst the quadratic stress terms are of size $O(\delta^{(1+2r-n)} = O(\mathrm{We}^{-(1+2r-n)/2})$. It is worth noting that the quadratic stress terms are larger, the same size and smaller than the linear stress terms if $0 < r < 1, r = 1$ and $r > 1$ respectively. These equations are subject to the outer matching conditions (4.13) with (4.14). The quadratic stress terms are recovered in an inner inner region and in order for the solution here to match to it, we are interested in limiting stress behaviour of the general form

$$\text{as } Y \to 0 \qquad \Psi \sim \hat{c}_0(X)Y^q, \;\; \bar{T}_{11} \sim \frac{\hat{c}_{11}(X)}{Y^2}, \;\; \bar{T}_{12} \sim \frac{\hat{c}_{12}(X)}{Y}, \;\; \bar{T}_{22} \sim -1 + \hat{c}_{22}(X). \tag{4.61}$$

Admissible $\hat{c}_0(X)$ and appropriate expressions for the $\hat{c}_{ij}(X)$ are given in appendix B of [1] for $q \geq 1$. The value of $q$ does not appear to be determined, although the values $q = 3/2$ and $q = n$ are expected to play important roles in general (particularly the $q = 3/2$ value). The source of this indeterminacy is the loss of the pressure gradient within the inner inner region, and as such additional information is required if the value of $q$ is to be fixed. However, proceeding generally we now consider another region in which the quadratic stress terms are retained at leading order, in order to recover viscometric behaviour. This inner inner region is given by the scalings

$$Y = \theta_2 \hat{Y}, \;\; \Psi = \theta_2^q \hat{\Psi}, \;\; \bar{T}_{11} = \frac{\hat{T}_{11}}{\theta_2^2}, \;\; \bar{T}_{12} = \frac{\hat{T}_{12}}{\theta_2}, \;\; \bar{T}_{22} = \hat{T}_{22}, \tag{4.62}$$

where $\theta_2 = \mathrm{We}^{-\frac{(1+2r-n)}{2(q+1)}}$. Since $n < \min(1+2r, 3)$ and $q > -1$ (whether $q = 3/2$ or $q = n$), then $\theta_2$ is small. For example,

$$\theta_2 = \begin{cases} \mathrm{We}^{-\frac{(1+2r-n)}{5}} & \text{if } q = 3/2, \\ \mathrm{We}^{-\frac{(1+2r-n)}{2(n+1)}} & \text{if } q = n. \end{cases}$$

The leading order equations in $X = O(1), \hat{Y} = O(1)$ are now

$$0 = \frac{\partial \hat{T}_{11}}{\partial X} + \frac{\partial \hat{T}_{12}}{\partial \hat{Y}}, \tag{4.63}$$

$$\left(\frac{\partial \hat{\Psi}}{\partial \hat{Y}}\frac{\partial \hat{T}_{11}}{\partial X} - \frac{\partial \hat{\Psi}}{\partial X}\frac{\partial \hat{T}_{11}}{\partial \hat{Y}} - 2\frac{\partial^2 \hat{\Psi}}{\partial \hat{Y}^2}\hat{T}_{12} - 2\frac{\partial^2 \hat{\Psi}}{\partial X \partial \hat{Y}}\hat{T}_{11}\right) + \hat{\kappa}\hat{T}_{11}^2 = 0, \tag{4.64}$$

$$\left(\frac{\partial \hat{\Psi}}{\partial \hat{Y}}\frac{\partial \hat{T}_{22}}{\partial X} - \frac{\partial \hat{\Psi}}{\partial X}\frac{\partial \hat{T}_{22}}{\partial \hat{Y}} + 2\frac{\partial^2 \hat{\Psi}}{\partial X^2}\hat{T}_{12} + 2\frac{\partial^2 \hat{\Psi}}{\partial X \partial \hat{Y}}\hat{T}_{22}\right) + \hat{\kappa}\hat{T}_{22}\hat{T}_{11} = -2\frac{\partial^2 \hat{\Psi}}{\partial X \partial \hat{Y}}, \tag{4.65}$$

$$\left(\frac{\partial \hat{\Psi}}{\partial \hat{Y}}\frac{\partial \hat{T}_{12}}{\partial X} - \frac{\partial \hat{\Psi}}{\partial X}\frac{\partial \hat{T}_{12}}{\partial \hat{Y}} + \frac{\partial^2 \hat{\Psi}}{\partial X^2}\hat{T}_{11} - \frac{\partial^2 \hat{\Psi}}{\partial \hat{Y}^2}\hat{T}_{22}\right) + \hat{\kappa}\hat{T}_{12}\hat{T}_{11} = \frac{\partial^2 \hat{\Psi}}{\partial \hat{Y}^2}. \tag{4.66}$$

These equations possess the wall viscometric behaviour (3.24) (adjusted for hat variables as appropriate). Matching to the limiting behaviour (4.61) of the inner solution gives the conditions

$$\text{as } \hat{Y} \to \infty \quad \hat{\Psi} \sim \hat{c}_0(X)\hat{Y}^q, \;\; \hat{T}_{11} \sim \frac{\hat{c}_{11}(X)}{\hat{Y}^2}, \;\; \hat{T}_{12} \sim \frac{\hat{c}_{12}(X)}{\hat{Y}}, \;\; \hat{T}_{22} \sim -1 + \hat{c}_{22}(X), \tag{4.67}$$

A noteworthy feature of these equations is that the pressure gradient is no longer present in the momentum equation at leading order. The omitted linear stress terms in this inner inner region are of size $O(\delta^{3-n}\theta_2^{1-q}) = O(\mathrm{We}^{-\frac{2-n+q+r(1-q)}{(q+1)}})$. From this we may deduce that they will enter at leading order when $r = r_2$ where

$$r_2 = \frac{(q+2-n)}{(q-1)} = \begin{cases} \frac{2}{(n-1)} & \text{if } q = n, \\ 7-2n & \text{if } q = 3/2, \end{cases} \tag{4.68}$$

This then defines a second and final critical value of $r$, which is noted to be greater than or equal to one.

### 4.3.2 The case $r = r_2$

At the critical value $r = r_2$, the balance for this case is given for

$$1 \le n < 3 \quad \text{and} \quad \delta = \mathrm{We}^{-1/2}. \tag{4.69}$$

We note that $\min(1+2r_2, 3) = 3$ gives the upper limit on the range for $n$. Similar to the previous case of $0 < r < r_2$ in section 4.3.1, in the inner region $X = O(1), Y = O(1)$ we again obtain

$$0 = -\frac{d\bar{p}}{dX} + \frac{\partial \bar{T}_{11}}{\partial X} + \frac{\partial \bar{T}_{12}}{\partial Y}, \tag{4.70}$$

$$\left(\frac{\partial \Psi}{\partial Y}\frac{\partial \bar{T}_{11}}{\partial X} - \frac{\partial \Psi}{\partial X}\frac{\partial \bar{T}_{11}}{\partial Y} - 2\frac{\partial^2 \Psi}{\partial Y^2}\bar{T}_{12} - 2\frac{\partial^2 \Psi}{\partial X \partial Y}\bar{T}_{11}\right) = 0, \tag{4.71}$$

$$\left(\frac{\partial \Psi}{\partial Y}\frac{\partial \bar{T}_{22}}{\partial X} - \frac{\partial \Psi}{\partial X}\frac{\partial \bar{T}_{22}}{\partial Y} + 2\frac{\partial^2 \Psi}{\partial X^2}\bar{T}_{12} + 2\frac{\partial^2 \Psi}{\partial X \partial Y}\bar{T}_{22}\right) = -2\frac{\partial^2 \Psi}{\partial X \partial Y}, \tag{4.72}$$

$$\left(\frac{\partial \Psi}{\partial Y}\frac{\partial \bar{T}_{12}}{\partial X} - \frac{\partial \Psi}{\partial X}\frac{\partial \bar{T}_{12}}{\partial Y} + \frac{\partial^2 \Psi}{\partial X^2}\bar{T}_{11} - \frac{\partial^2 \Psi}{\partial Y^2}\bar{T}_{22}\right) = \frac{\partial^2 \Psi}{\partial Y^2}. \tag{4.73}$$

as the leading order equations together with the limiting behaviour (4.61). The omitted linear stress terms in this region are again of size $O(\delta^{3-n}) = O(\mathrm{We}^{-(3-n)/2})$, whilst the quadratic stress terms are now of size $O(\delta^{(1+2r_2-n)}) = O(\mathrm{We}^{-(q+1)(3-n)/(q-1)})$.

The linear and quadratic stress terms are recovered within the inner inner region, the scalings for which are given by

$$Y = \theta_2 \hat{Y}, \quad \Psi = \theta_2^q \hat{\Psi}, \quad \bar{T}_{11} = \frac{\hat{T}_{11}}{\theta_2^2}, \quad \bar{T}_{12} = \frac{\hat{T}_{12}}{\theta_2}, \quad \bar{T}_{22} = \hat{T}_{22}, \tag{4.74}$$

where $\theta_2 = \mathrm{We}^{-\frac{(1+2r_2-n)}{2(q+1)}} = \mathrm{We}^{-\frac{(3-n)}{2(q-1)}}$. Since $n < 3$ and $q > -1$ then $\theta_2$ is small. The leading order equations in $X = O(1), \hat{Y} = O(1)$ are now

$$0 = \frac{\partial \hat{T}_{11}}{\partial X} + \frac{\partial \hat{T}_{12}}{\partial \hat{Y}}, \tag{4.75}$$

$$\hat{T}_{11} + \left( \frac{\partial \hat{\Psi}}{\partial \hat{Y}} \frac{\partial \hat{T}_{11}}{\partial X} - \frac{\partial \hat{\Psi}}{\partial X} \frac{\partial \hat{T}_{11}}{\partial \hat{Y}} - 2\frac{\partial^2 \hat{\Psi}}{\partial \hat{Y}^2} \hat{T}_{12} - 2\frac{\partial^2 \hat{\Psi}}{\partial X \partial \hat{Y}} \hat{T}_{11} \right) + \hat{\kappa} \hat{T}_{11}^2 = 0, \tag{4.76}$$

$$\hat{T}_{22} + \left( \frac{\partial \hat{\Psi}}{\partial \hat{Y}} \frac{\partial \hat{T}_{22}}{\partial X} - \frac{\partial \hat{\Psi}}{\partial X} \frac{\partial \hat{T}_{22}}{\partial \hat{Y}} + 2\frac{\partial^2 \hat{\Psi}}{\partial X^2} \hat{T}_{12} + 2\frac{\partial^2 \hat{\Psi}}{\partial X \partial \hat{Y}} \hat{T}_{22} \right) + \hat{\kappa} \hat{T}_{22} \hat{T}_{11} = -2\frac{\partial^2 \hat{\Psi}}{\partial X \partial \hat{Y}}, \tag{4.77}$$

$$\hat{T}_{12} + \left( \frac{\partial \hat{\Psi}}{\partial \hat{Y}} \frac{\partial \hat{T}_{12}}{\partial X} - \frac{\partial \hat{\Psi}}{\partial X} \frac{\partial \hat{T}_{12}}{\partial \hat{Y}} + \frac{\partial^2 \hat{\Psi}}{\partial X^2} \hat{T}_{11} - \frac{\partial^2 \hat{\Psi}}{\partial \hat{Y}^2} \hat{T}_{22} \right) + \hat{\kappa} \hat{T}_{12} \hat{T}_{11} = \frac{\partial^2 \hat{\Psi}}{\partial \hat{Y}^2}. \tag{4.78}$$

At the wall, we now have the viscometric behaviour

$$\begin{aligned}
\hat{\Psi} &= \frac{1}{2} a(X) Y^2 - \left( \frac{(1 + 3\hat{\kappa} a_{11}(X) - 6\hat{\kappa}^2 a_{11}(X)^2) a(X)^3 a'(X)}{3 a_{11}(X)(1 + 3\hat{\kappa} a_{11}(X))(1 + \hat{\kappa} a_{11}(X))^4} \right) Y^3 + O(Y^4), \\
\bar{T}_{11} &= a_{11}(X) - \left( \frac{2(5 + 6\hat{\kappa} a_{11}(X) - 12\hat{\kappa}^2 a_{11}(X)^2) a(X)^2 a'(X)}{(1 + \hat{\kappa} a_{11}(X))(1 + 3\hat{\kappa} a_{11}(X))^2} \right) Y + O(Y^2), \\
\bar{T}_{12} &= \frac{a(X)}{(1 + \hat{\kappa} a_{11}(X))} - \left( \frac{8(1 + 4\hat{\kappa} a_{11}(X) + 3\hat{\kappa}^2 a_{11}(X)^2) a(X)^3 a'(X)}{a_{11}(X)(1 + \hat{\kappa} a_{11}(X))^4 (1 + 3\hat{\kappa} a_{11}(X))^2} \right) Y + O(Y^2), \\
\bar{T}_{22} &= -\frac{2a'(X)}{(1 + \hat{\kappa} a_{11}(X))} Y + O(Y^2), \qquad \text{as } Y \to 0
\end{aligned} \tag{4.79}$$

with $a_{11}(X)$ satisfying (4.27). Allowing for a change in notation to hat variables, (4.79) may be deduced from (4.25) by using the value of $b(X)$ that makes $\bar{p}'(X) = 0$ in (4.26). The matching conditions with the inner solution are (4.67).

### 4.3.3 The case $r > r_2$

The structure of the previous subsection persists with the same scalings (4.56) and (4.69) for the inner and inner inner regions holding. The leading order equations in the inner region are again (4.70)–(4.73), whilst those for the inner inner region are (4.75)–(4.78) with $\hat{\kappa}$ set to zero. The quadratic stress terms within the inner inner region can be verified to be $O(\mathrm{We}^{-(r-r_2)/(rr_2)})$. This then recovers the third and final UCM structure.

## 4.4 Summary

Figure 5 conveniently summarises the nine structures considered in this section in terms of the two exponents $r$ and $n$. We can move smoothly between the various structures by taking the appropriate limit in $n$ or $r$, provided care is taken in the identifying the correct terms to be recovered (or lost). In the limit $r \to 0$ the single layer structure recovers the $n = 1$ structure of the $\kappa = O(1)$ case in section 3.1. However, the type I boundary layer actually breaks down in this limit where the inner region no longer remains small, the range $r = 0, n > 1$ being the extent of its validity. For the type II structure, the line $n = 1, r > 0$ is attainable but does provide a restriction on the extension of these types of structures to regions with $n < 1$. The single layer structures clearly play a central role, with the double layers structures bifurcating from them. Importantly though, it is the three distinct balances obtained for the single layer structure that manifest themselves in the inner inner layers of the two double layer structures. These three single layer structures represent the three viscometric behaviours for the PTT model that can occur for different sizes of $\kappa$ relative to We. In the UCM model, only one viscometric behaviour is possible giving rise to a unique single layer structure.

It is worth commenting upon the case $n = 2$ in which we obtain a limiting shear rate from the core. Figure 5 indicates that we obtain the type I double layer structure for $0 < r < 1/2$, the single layer structure when $r = 1/2$ and the type II double layer structure for $r > 1/2$.

As regards the single boundary layer structure, the analysis of section 4.1 clearly indicates that there is a unique value of $n$ depending on the value of $r$ (which will fixed for a given situation and in the range $r > 0$). In other words we must accept this value of $n$, which we note is generally different from 2. We also note that if in contrast we imposed $n = 2$, then we generally lose the pressure gradient for single layer structures. Consequently the momentum equation in the boundary layer becomes degenerate and imposes a restriction on possible stream function behaviours from the core. This explained more fully in Appendix D.

For a given situation in which $\kappa = o(1)$, Figure 5 may be used as follows. The relative size of $\kappa$ to $\mathrm{We}^{-1}$ will be fixed and hence an appropriate $r > 0$ and $\hat{\kappa}$ can be determined. For this fixed value of $r$, Figure 5 then indicates the boundary layer structures that are expected according to the value of $n > 1$. The exponent $n$ is uniquely determined for a single layer structure whilst it may take ranges for the two double layer structures. This then categorises the likely structures we may expect at the wall and when (with respect to $n$) we will obtain them. Which of these structures actually manifests itself, will depend on the particular situation i.e. the particular global as well as local geometry, the presence of singularities and separating streamlines, stability of solutions to these structures etc. The intention of this work was simply to classify the possibilities.

## 5. Discussion

Here we have classified the high Weissenberg boundary layer structures for the PTT model. This has been done for limiting core behaviours in separable form, although the structures described are expected to occur for more general limiting behaviour. The PTT model adds a quadratic stress term of a specific form to the UCM model constitutive equations and it is the effect of such a term on possible boundary layer structures that has been quantified.

When the PTT model parameter $\kappa$ is $O(1)$ then strictly only one balance occurs in the constitutive equations as described in section 3. The effect of the quadratic stress is certainly influential in limiting the number of dominant balances and moreover restricts the growth of the stream function to essentially a linear function in the far-field of the boundary layer. This contrasts with the situation when $\kappa = o(1)$. Now a variety of structures are possible as categorised in section 4. Focusing on the single layer structures, the balance of the $\kappa = O(1)$ flows holds for $\kappa = O(\mathrm{We}^{-r})$ with $0 < r < 1$. At $\kappa = O(\mathrm{We}^{-1})$ the linear stress terms now enter the boundary layer balance and for $\kappa = O(\mathrm{We}^{-r})$ with $r > 1$ then the quadratic stress terms are negligible at leading order and the UCM single layer structure is obtained. Interestingly, the far-field growth of the stream function increases steadily as $\kappa$ decreases. More precisely, in our boundary variables

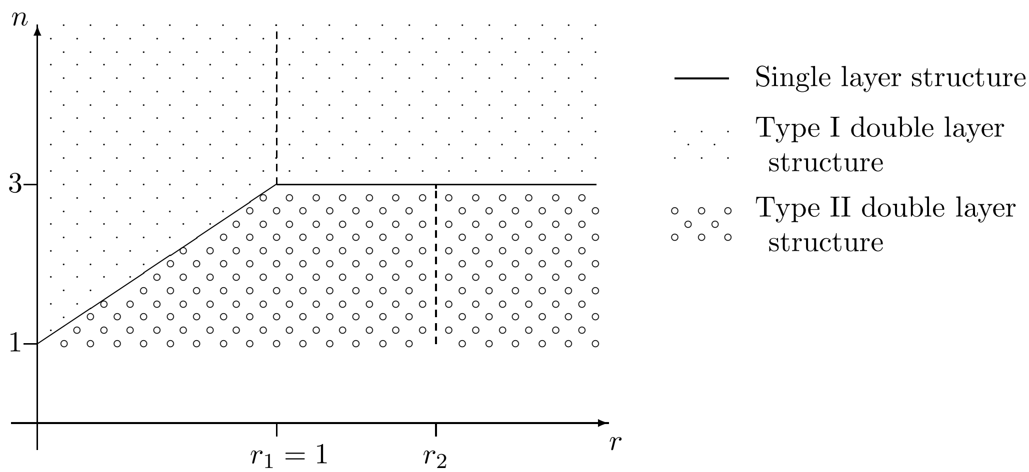


Figure 5: A summary of the exponents $n$ and $r$ and their values for the $\kappa = o(1)$ boundary layer structures. For a given $r$, a unique $n$ is determined for single layer structures, whilst a range for $n$ is obtained for the two double layer structures. For each type of structure (single layer, double layer I or II) there are three cases for $r$ representing balances that give the three distinct viscometric behaviours. In the single and type I double layer structure these are $0 < r < 1, r = 1, r > 1$ whilst for the type II double layer structure these are $0 < r < r_2, r = r_2, r > r_2$.

$\Psi = O(Y^{1+2r})$ for $0 < r < 1$ and $\Psi = O(Y^3)$ for $r \geq 1$ as $Y \to \infty$. Essentially this is one of the main effects of the quadratic stress terms and is consistent with the PTT model capturing shear thinning effects.

A comment on the determination of the exponent $n$ is appropriate in that it highlights an important difference between the single and two double boundary layer structures. For the single layer structure, $n$ is determined uniquely for a given $r$. This contrasts with both double layer structures, where for the same $r$ a range of $n$ is now possible. Thus, for the single layer structures, $n$ is determined purely by local considerations. In contrast, for both double layer structures the appropriate value of $n$ is no longer apparent and must be provided by the outer core flow i.e. $n$ for these structures requires global information.

We note that the boundary thicknesses here aren't necessarily significantly different from those in the UCM case. In fact for the single layer structures which maintain their pressure gradients then the boundary layers are the same thickness namely $O(\mathrm{We}^{-1/2})$ irrespective of the size of $\kappa$. However, we remark that the presence of a Newtonian solvent stress in the momentum equation, radically alters the solution behaviour within both the core flows and boundary layer structures. We will still have the generic three viscometric behaviours and consequent boundary layer balances between terms in the constitutive equations. However, limiting core behaviours and boundary layer scalings will be expected to change to those given here. It is worth remarking that [3] considered the case $n = 2$ and deduced that the PTT (single) boundary layers are of thickness $O(\mathrm{We}^{-1/3})$ in $\kappa = O(1)$ flows and compare to thinner UCM (single) boundary layers of thickness $O(\mathrm{We}^{-1})$ when both models receive a stream function with quadratic behaviour (in the normal coordinate to the boundary) from the core. This comparison is on a like for like basis and as we have discussed in section 4.4 is not immediately applicable to the situation we have been considering in this paper.

## References

[1] J.D. Evans, High Weissenberg number boundary layer structures for UCM fluids. Submitted to *J. Non-Newtonian Fluid Mech.* (2005).

[2] H. Giesekus. A unified approach to a variety of constitutive models for polymer fluids based on the concept of configuration dependent molecular mobility. *Rheol. Acta.* **21** (1982), 366–375.

[3] T. Hagen and M. Renardy, Boundary layer analysis of the Phan-Thien-Tanner and Giesekus model in high Weissenberg number flow. *J. Non-Newtonian Fluid Mech.* **73** (1997), 181–189.

[4] J. Kevorkian and J.D. Cole, *Perturbation methods in applied mathematics*, Springer-Verlag, New-York, 1981.

[5] N. Phan-Thien and R.I. Tanner. A new constitutive equation derived from network theory. *J.Non-Newtonian Fluid Mech.* **2** (1977), 353–365.

[6] M. Renardy, High Weissenberg number boundary layers for the upper convected Maxwell fluid. *J. Non-Newtonian Fluid Mech.* **68** (1997), 125–132.

[7] M. Renardy, The high Weissenberg number limit of the UCM model and the Euler equations *J. Non-Newtonian Fluid Mech.* **69** (1997), 293–301.

[8] M. Renardy, *Mathematical Analysis of Viscoelastic Flows*, SIAM, 2000.

## Appendix A. Limiting core behaviour for the $\kappa = O(1)$ flows

In component form, (3.1) is

$$\frac{\partial\psi}{\partial y}\frac{\partial T_{11}}{\partial x} - \frac{\partial\psi}{\partial x}\frac{\partial T_{11}}{\partial y} - 2\frac{\partial^2\psi}{\partial y^2}T_{12} - 2\frac{\partial^2\psi}{\partial x\partial y}T_{11} + \kappa T_{11}(T_{11}+T_{22}) = 0, \tag{A.1}$$

$$\frac{\partial\psi}{\partial y}\frac{\partial T_{22}}{\partial x} - \frac{\partial\psi}{\partial x}\frac{\partial T_{22}}{\partial y} + 2\frac{\partial^2\psi}{\partial x^2}T_{12} + 2\frac{\partial^2\psi}{\partial x\partial y}T_{22} + \kappa T_{22}(T_{11}+T_{22}) = 0, \tag{A.2}$$

$$\frac{\partial\psi}{\partial y}\frac{\partial T_{12}}{\partial x} - \frac{\partial\psi}{\partial x}\frac{\partial T_{12}}{\partial y} + \frac{\partial^2\psi}{\partial x^2}T_{11} - \frac{\partial^2\psi}{\partial y^2}T_{22} + \kappa T_{12}(T_{11}+T_{22}) = 0, \tag{A.3}$$

For the behaviour (3.2), we consider solutions of the form

$$T_{11} = c_{11}(x)y^{n-1}, \quad T_{12} = c_{12}(x)y^n, \quad T_{22} = c_{22}(x)y^{n+1}, \tag{A.4}$$

where the exponents for the $y$ dependence of the extra-stresses follow from requiring a non-trivial balance in (A.1)–(A.3). [2] To leading order (in $y$) we obtain

$$nc_0(x)c_{11}' - (3n-1)c_0'(x)c_{11} - 2n(n-1)c_0(x)c_{12} + \kappa c_{11}^2 = 0, \tag{A.5}$$

$$nc_0(x)c_{22}' + (n-1)c_0'(x)c_{22} + 2c_0''(x)c_{12} + \kappa c_{11}c_{22} = 0, \tag{A.6}$$

$$nc_0(x)c_{12}' - nc_0'(x)c_{12} + c_0''(x)c_{11} - n(n-1)c_0(x)c_{22} + \kappa c_{12}c_{11} = 0. \tag{A.7}$$

Here and in the rest of this appendix, $'$ denotes $d/dx$. For later reference, the components of the momentum equation are

$$\mathrm{Re}nc_0c_0'y^{2(n-1)} = -\frac{\partial p}{\partial x} + y^{n-1}\left(c_{11}' + nc_{12}\right), \tag{A.8}$$

$$\mathrm{Re}n(c_0'^2 - c_0c_0'')y^{2n-1} = -\frac{\partial p}{\partial y} + y^n\left(c_{12}' + (n+1)c_{22}\right). \tag{A.9}$$

Following [7] and [3], we may express the extra-stresses (A.4) in terms of their natural basis. Explicitly, as the boundary is approached this formulation has the limiting form

$$T_{11} = \lambda u^2, \quad T_{12} = \lambda uv + \mu, \quad T_{22} = \lambda v^2 + \frac{2\mu v}{u} + \frac{\nu}{u^2},$$

where $u = \dfrac{\partial\psi}{\partial y}, v = -\dfrac{\partial\psi}{\partial x}$ are the usual velocity components. (In contrast to [3] we have not scaled $\lambda$ and $\nu$ with $\kappa^2$.) Here then we may write

$$\lambda(x,y) = \lambda_0(x)y^{1-n}, \quad \mu(x,y) = \mu_0(x)y^n, \quad \nu(x,y) = \nu_0(x)y^{3n-1},$$

where

$$c_{11}(x) = n^2c_0(x)^2\lambda_0(x), \tag{A.10}$$

$$c_{12}(x) = -\frac{c_0'(x)}{nc_0(x)}c_{11}(x) + \mu_0(x), \tag{A.11}$$

$$c_{22}(x) = \left(\frac{c_0'(x)}{nc_0(x)}\right)^2 c_{11}(x) - \frac{2c_0'(x)}{nc_0(x)}\mu_0(x) + \frac{\nu_0(x)}{n^2c_0(x)^2}. \tag{A.12}$$

The equations (A.5)–(A.7) are a third-order linear system of ODEs for the unknowns $c_{11}, c_{12}, c_{22}$. We now record explicit solutions for these expressions in the cases $n = 1$ and $n > 1$.

[2] It is noteworthy that in the limit $y \to 0$, $T_{22} \ll T_{11}$ and so the last terms on the left-hand-side of (A.1)–(A.3) may be dropped. The remaining terms then admit invariance under the general scaling group

$$x = \alpha\bar{x}, \quad y = \beta\bar{y}, \quad \psi = \gamma\bar{\psi}, \quad T_{11} = \frac{\gamma}{\alpha\beta}\bar{T}_{11}, \quad T_{12} = \frac{\gamma}{\alpha^2}\bar{T}_{12}, \quad T_{22} = \frac{\gamma\beta}{\alpha^3}\bar{T}_{22},$$

for $\alpha, \beta, \gamma \in \Re$. In particular, taking $\alpha = 1, \beta = y$ and $\gamma = \beta^n$ due to (3.2), we then recover the scalings in y given in (A.4).

### A.1 The case $n = 1$ with general $c_0(x)$

In this case we have the exact solution

$$c_{11}(x) = \frac{c_1 c_0(x)^2}{(\kappa c_1 I(x) + 1)}, \tag{A.13}$$

$$c_{12}(x) = \frac{c_0(x)\left(-c_1 c_0'(x) + c_2\right)}{(\kappa c_1 I(x) + 1)}, \tag{A.14}$$

$$c_{22}(x) = \frac{\left(c_1 c_0'(x)^2 - 2c_2 c_0'(x) + c_3\right)}{(\kappa c_1 I(x) + 1)}, \tag{A.15}$$

where

$$I(x) = \int c_0(x)dx. \tag{A.16}$$

The constant of integration in $I(x)$ can be absorbed into the arbitrary constants $c_1, c_2, c_3$. Relevant to the pressure gradient, we record the quantity

$$c_{11}'(x) + c_{12}(x) = \frac{c_0(x)\left(\left(c_1 c_0'(x) + c_2\right)(\kappa c_1 I(x) + 1) - \kappa c_1^2 c_0(x)^2\right)}{(\kappa c_1 I(x) + 1)^2}.$$

In terms of the natural stress variables we have the identification

$$\lambda_0(x) = \frac{c_{11}(x)}{c_0(x)^2} = \frac{c_1}{(\kappa c_1 I(x) + 1)}, \tag{A.17}$$

$$\mu_0(x) = \frac{c_0(x)c_2}{(\kappa c_1 I(x) + 1)}, \tag{A.18}$$

$$\nu_0(x) = \frac{c_0(x)^2 c_3}{(\kappa c_1 I(x) + 1)}. \tag{A.19}$$

The constraint $\lambda\nu = \mu^2$ is now satisfied if $c_2^2 = c_1 c_3$. This was the condition noted in [7] for $\mathbf{T}$ to be rank one tensor in the outer core region for the UCM model. It appears that this is also true for the PTT model when $\kappa \neq 0$.

In the case $\kappa = 0$, we recover the results obtained in [1] for the UCM model. We remark that for $\kappa \neq 0$, it no longer holds that $\lambda, \mu, \nu$ can be functions of the stream function.

In the particular case $c_0(x) = C_0 x^m$ we obtain for $m \neq -1$

$$c_{11}(x) = \frac{c_1 C_0^2 x^{2m}}{\left(\frac{\kappa c_1 C_0}{1+m} x^{1+m} + 1\right)}, \tag{A.20}$$

$$c_{12}(x) = \frac{C_0 x^m \left(-m c_1 x^{m-1} + c_2\right)}{\left(\frac{\kappa c_1 C_0}{1+m} x^{1+mn} + 1\right)}, \tag{A.21}$$

$$c_{22}(x) = \frac{\left(c_1 C_0^2 m^2 x^{2m-2} - 2c_2 C_0 m x^{m-1} + c_3\right)}{\left(\frac{\kappa c_1 C_0}{1+m} x^{1+m} + 1\right)}, \tag{A.22}$$

whilst for $m = -1$ we have

$$c_{11}(x) = \frac{c_1 C_0^2 x^{-2}}{(\kappa c_1 C_0 \ln x + 1)}, \tag{A.23}$$

$$c_{12}(x) = \frac{C_0 x^{-1}\left(c_1 C_0 x^{-2} + c_2\right)}{(\kappa c_1 C_0 \ln x + 1)}, \tag{A.24}$$

$$c_{22}(x) = \frac{\left(c_1 C_0^2 x^{-4} + 2c_2 C_0 x^{-2} + c_3\right)}{(\kappa c_1 C_0 \ln x + 1)}, \tag{A.25}$$

## A.2 The case $n > 1$ with general $c_0(x)$

In this case the momentum equation gives the relationship (3.7) between $c_{11}$ and $c_{12}$. Using this (A.5)–(A.7) may be integrated to give

$$c_{11}(x) = \frac{c_0(x)^{\frac{3n-1}{3n-2}}}{\kappa I_n(x) + c_1},$$

$$c_{12}(x) = \frac{\left(c_0(x)^{\frac{1}{3n-2}}\left(\kappa c_0(x)^{\frac{1}{3n-2}}\right) - (3n-1)(\kappa I_n(x) + c_1)c_0'(x)\right)}{(3n-2)n(\kappa I_n(x) + c_1)^2}$$

$$c_{22}(x) = \frac{\left(c_0(x)^{\frac{3n-1}{3n-2}}(nc_0''(x) - \kappa c_{11}'(x)) + n(\kappa I_n(x) + c_1)(c_0'(x)c_{11}'(x) - c_0(x)c_{11}''(x))\right)}{n^2(n-1)c_0(x)(\kappa I_n(x) + c_1)}$$

where

$$I_n(x) = \int \frac{c_0(x)^{\frac{1}{3n-2}}}{(3n-2)} dx \tag{A.26}$$

and admissible $c_0(x)$ and $n$ must satisfy the integro-differential equation

$$\begin{aligned} n\bigg(& n(3n-2)^2 c_0(x)^2 c_0'''(x) - (3n-2)(9n^2 - 12n + 2)c_0(x)c_0'(x)c_0''(x) \\ &+6(3n-1)(n-1)^2 c_0'(x)^3\bigg)(\kappa I_n(x) + c_1)^3 + \bigg(2n(n-2)(3n-2)c_0''(x)c_0(x)^{\frac{3(2n-1)}{(3n-2)}} \\ &-2(3n^3 - 9n^2 + 10n - 2)c_0'(x)^2 c_0(x)^{\frac{(3n-1)}{(3n-2)}}\bigg)\kappa(\kappa I_n(x) + c_1)^2 \\ -6n(n-2)&c_0'(x)c_0(x)^{\frac{2(3n-1)}{(3n-2)}}\kappa^2(\kappa I_n(x) + c_1) + 2(n-2)\kappa^3 c_0(x)^{\frac{3(3n-1)}{(3n-2)}} = 0. \end{aligned} \tag{A.27}$$

There is clearly a critical case when $n = 2/3$, which will not be considered here since it is outside our range of interest for $n$.

In the particular case $c_0(x) = C_0 x^{mn}$, we find that the only general solution in which $c_1$ is left arbitrary is when $n = 2, m = 0$.

## Appendix B. The natural stress basis for the single layer structures

It is worth recording these boundary layer equations that arise in the single layer structures of sections 3.1 and 4.1, in terms of the natural stress basis variables $\lambda, \nu, \mu$ given by

$$\bar{T}_{11} = \lambda u^2, \quad \bar{T}_{12} = \lambda uv + \mu, \quad \bar{T}_{22} = -1 + \lambda v^2 + \frac{2\mu v}{u} + \frac{\nu}{u^2},$$

where $u = \dfrac{\partial \Psi}{\partial Y}, v = -\dfrac{\partial \Psi}{\partial X}$ are the velocity components.

### B.1 The $n = 1$ and $n = 1 + 2r$ structures

The equations (3.16)–(3.19) and (4.16)–(4.19) become

$$0 = -\frac{d\bar{p}}{dX} + \left(\frac{\partial \Psi}{\partial Y}\right)\frac{\partial}{\partial X}\left(\lambda \frac{\partial \Psi}{\partial Y}\right) - \left(\frac{\partial \Psi}{\partial X}\right)\frac{\partial}{\partial Y}\left(\lambda \frac{\partial \Psi}{\partial Y}\right) + \frac{\partial \mu}{\partial Y}, \tag{B.1}$$

$$\left(\frac{\partial \Psi}{\partial Y}\right)^2 \left(\frac{\partial \Psi}{\partial Y}\frac{\partial \lambda}{\partial X} - \frac{\partial \Psi}{\partial X}\frac{\partial \lambda}{\partial Y} + \lambda + \kappa\lambda^2 \left(\frac{\partial \Psi}{\partial Y}\right)^2\right) - 2\frac{\partial^2 \Psi}{\partial Y^2}\mu = 0, \tag{B.2}$$

$$\left(\frac{\partial \Psi}{\partial X}\right)^2 \left(\frac{\partial \Psi}{\partial Y}\frac{\partial \mu}{\partial X} - \frac{\partial \Psi}{\partial X}\frac{\partial \mu}{\partial Y} + \mu + \kappa\lambda\mu \left(\frac{\partial \Psi}{\partial Y}\right)^2\right) - \frac{\partial^2 \Psi}{\partial Y^2}\nu = 0, \tag{B.3}$$

$$\frac{\partial \Psi}{\partial Y}\frac{\partial \nu}{\partial X} - \frac{\partial \Psi}{\partial X}\frac{\partial \nu}{\partial Y} + \kappa\lambda \left(\frac{\partial \Psi}{\partial Y}\right)^2 \left(\nu - \left(\frac{\partial \Psi}{\partial Y}\right)^2\right) = 0. \tag{B.4}$$

The matching condition with the outer gives the behaviour

$$\text{as } Y \to \infty \qquad \Psi \sim c_0(X)Y^n, \quad \lambda \sim \lambda_0(X)Y^{2(1-n)}, \quad \mu \sim \mu_0(X)Y, \quad \nu \sim \nu_0(X)Y^{2n}, \tag{B.5}$$

with

$$\bar{p}'(X) = n^2(c_0(X)^2\lambda_0(X))' - nc_0(X)c_0'(X)\lambda_0(X) + \mu_0(X) - Re c_0(X)c_0'(X)\delta_{n1}. \tag{B.6}$$

At the wall we have the behaviour

$$\begin{aligned} \text{as } Y \to 0 \qquad & \Psi = \kappa a(X)^3Y^2 + \kappa a(X)^4 b(X)Y^3 + O(Y^4), \\ & \lambda = \frac{Y^{-2}}{2\kappa^2 a(X)^4} - \left(\frac{a(X)b(X) + a'(X)}{2\kappa^2 a(X)^4}\right)Y^{-1} + O(1), \\ & \mu = a(X) + a(X)(a(X)b(X) - 3a'(X))Y + O(Y^2), \\ & \nu = 4\kappa^2 a(X)^6 Y^2 + 12\kappa^2 a(X)^6 \left(a(X)b(X) - a'(X)\right)Y^3 + O(Y^4), \end{aligned} \tag{B.7}$$

with

$$\bar{p}'(X) = a(X)a'(X) + b(X). \tag{B.8}$$

In the matching behaviour (B.5) we have $\lambda_0(X), \mu_0(X), \nu_0(X)$ given by (A.17)–(A.19) for (3.16)–(3.19) with $n = 1$ and the expressions in appendix A in [1] when (4.16)–(4.19) and $n = 1 + 2r$ are being considered.

### B.2 The $n = 3$ structure

The equations (4.21)–(4.24) become

$$0 = -\frac{d\bar{p}}{dX} + \left(\frac{\partial \Psi}{\partial Y}\right)\frac{\partial}{\partial X}\left(\lambda \frac{\partial \Psi}{\partial Y}\right) - \left(\frac{\partial \Psi}{\partial X}\right)\frac{\partial}{\partial Y}\left(\lambda \frac{\partial \Psi}{\partial Y}\right) + \frac{\partial \mu}{\partial Y}, \tag{B.9}$$

$$\left(\frac{\partial \Psi}{\partial Y}\right)^2 \left(\frac{\partial \Psi}{\partial Y}\frac{\partial \lambda}{\partial X} - \frac{\partial \Psi}{\partial X}\frac{\partial \lambda}{\partial Y} + \lambda + \kappa\lambda^2 \left(\frac{\partial \Psi}{\partial Y}\right)^2\right) - 2\frac{\partial^2 \Psi}{\partial Y^2}\mu = 0, \tag{B.10}$$

$$\left(\frac{\partial \Psi}{\partial X}\right)^2 \left(\frac{\partial \Psi}{\partial Y}\frac{\partial \mu}{\partial X} - \frac{\partial \Psi}{\partial X}\frac{\partial \mu}{\partial Y} + \mu + \kappa\lambda\mu \left(\frac{\partial \Psi}{\partial Y}\right)^2\right) - \frac{\partial^2 \Psi}{\partial Y^2}\nu = 0, \tag{B.11}$$

$$\frac{\partial \Psi}{\partial Y}\frac{\partial \nu}{\partial X} - \frac{\partial \Psi}{\partial X}\frac{\partial \nu}{\partial Y} + \nu + \kappa\lambda \left(\frac{\partial \Psi}{\partial Y}\right)^2 \left(\nu - \left(\frac{\partial \Psi}{\partial Y}\right)^2\right) - \left(\frac{\partial \Psi}{\partial Y}\right)^2 = 0. \tag{B.12}$$

The matching condition with the outer gives the behaviour

$$\text{as } Y \to \infty \qquad \Psi \sim c_0(X)Y^3, \quad \lambda \sim \lambda_0(X)Y^{-4}, \quad \mu \sim \mu_0(X)Y, \quad \nu \sim \nu_0(X)Y^6, \tag{B.13}$$

with

$$\bar{p}'(X) = 9(c_0(X)^2\lambda_0(X))' - 3c_0(X)c_0'(X)\lambda_0(X) + \mu_0(X). \tag{B.14}$$

In the behaviour (B.13) we have $\lambda_0(X), \mu_0(X), \nu_0(X)$ given by the expressions in appendix A of [1].

At the wall we have the behaviour

$$\begin{aligned}
\Psi &= \frac{1}{2}a(X)Y^2 + \frac{1}{6}b(X)Y^3 + O(Y^4),\\
\lambda &= \frac{a_{11}(X)}{a(X)^2}Y^{-2} + \left(\frac{a_{11}(X)(1-\hat{\kappa}a_{11}(X))b(X)}{a(X)^3(1+3\hat{\kappa}a_{11}(X))} - \frac{6a'(X)}{(1+\hat{\kappa}a_{11}(X))(1+3\hat{\kappa}a_{11}(X))^2}\right)Y^{-1} + O(1),\\
\mu &= \frac{a(X)}{(1+\hat{\kappa}a_{11}(X))} + \left(\frac{b(X)}{(1+3\hat{\kappa}a_{11}(X))} - \frac{2(2+7\hat{\kappa}a_{11}(X)+9\hat{\kappa}^2a_{11}(X)^2)a(X)^3a'(X)}{a_{11}(X)(1+3\hat{\kappa}a_{11}(X))^2(1+\hat{\kappa}a_{11}(X))^4}\right)Y + O(Y^2),\\
\nu &= 4\kappa^2a(X)^6Y^2 + a(X)\left(b(X) - \frac{a(X)a'(X)}{(1+\hat{\kappa}a_{11}(X))}\right)Y^3 + O(Y^4) \qquad \text{as } Y \to 0
\end{aligned} \tag{B.15}$$

with $\bar{p}'(X)$ given by (4.26).

## Appendix C. Limiting behaviour of the inner equations (4.29)–(4.32)

Seeking solutions in the form

$$\Psi = \bar{c}_0(X)Y, \quad \bar{T}_{11} = \bar{c}_{11}(X), \quad \bar{T}_{12} = \bar{c}_{12}(X)Y, \quad \bar{T}_{22} = \bar{c}_{22}(X)Y^2,$$

then (4.46)–(4.48) give

$$\bar{c}_0(X)\bar{c}_{11}' - 2\bar{c}_0'(X))\bar{c}_{11} + \bar{c}_{11}\left(1 + \hat{\kappa}\bar{c}_{11}\right) = 0, \tag{C.1}$$

$$\bar{c}_0(X)\bar{c}_{22}' + 2\bar{c}_0''(X)\bar{c}_{12} + \bar{c}_{22}\left(1 + \hat{\kappa}\bar{c}_{11}\right) = 0, \tag{C.2}$$

$$\bar{c}_0(X)\bar{c}_{12}' + \bar{c}_0''(X)\bar{c}_{11} - \bar{c}_0'(X)\bar{c}_{12} + \bar{c}_{12}\left(1 + \hat{\kappa}\bar{c}_{11}\right) = 0. \tag{C.3}$$

Here $'$ denotes $d/dX$. In this case we have the exact solution

$$\bar{c}_{11}(X) = \frac{\bar{C}_1\bar{c}_0(X)^2e^{-\bar{I}(X)}}{\left(1 + \bar{C}_1\hat{\kappa}\int c_0(X)e^{-\bar{I}(X)}dX\right)}, \tag{C.4}$$

$$\bar{c}_{12}(X) = -\frac{(\bar{C}_1c_0'(X) - \bar{C}_2)c_0(X)e^{-\bar{I}(X)}}{\left(1 + \bar{C}_1\hat{\kappa}\int c_0(X)e^{-\bar{I}(X)}dX\right)}, \tag{C.5}$$

$$\bar{c}_{22}(X) = \frac{\left(\bar{C}_1\bar{c}_0'(X)^2 - 2\bar{C}_2\bar{c}_0'(X) + \bar{C}_3\right)e^{-\bar{I}(x)}}{\left(1 + \bar{C}_1\hat{\kappa}\int c_0(X)e^{-\bar{I}(X)}dX\right)}, \tag{C.6}$$

where

$$\bar{I}(X) = \int \bar{c}_0(X)^{-1}dX \tag{C.7}$$

and $\bar{C}_1, \bar{C}_2, \bar{C}_3$ are arbitrary constants. The momentum equation (4.45) becomes

$$\frac{d\bar{p}}{dX} = \bar{c}_0(X)e^{-\bar{I}(x)}\left(\frac{\left(\bar{C}_1(\bar{c}_0'(X)-1)+\bar{C}_2\right)}{\left(1+\bar{C}_1\hat{\kappa}\int c_0(X)e^{-\bar{I}(X)}dX\right)} - \frac{\hat{\kappa}\bar{C}_1^2 c_0(X)^2 e^{-\bar{I}(X)}}{\left(1+\bar{C}_1\hat{\kappa}\int c_0(X)e^{-\bar{I}(X)}dX\right)^2}\right). \tag{C.8}$$

We note that when $\bar{c}_0(X) = C_0 X^{mn}$ then

$$\bar{I}(X) = \begin{cases} \frac{X^{1-mn}}{C_0(1-mn)} & \text{if } mn \neq 1, \\ \frac{\ln X}{C_0} & \text{if } mn = 1, \end{cases}$$

and the integrals occuring in (C.4)–(C.6) can be expressed in terms of Whittaker M functions if $mn \neq 1$ or suitable powers of $X$ if $mn = 1$.

## Appendix D. Single boundary layer structures with small pressure gradients

Let us begin here by considering the more general limiting outer core behaviour

$$\psi \sim c_0(x)y^n, \quad T_{11} \sim c_{11}(x)y^s, \quad T_{12} \sim c_{12}(x)y^{s+1}, \quad T_{22} \sim c_{22}(x)y^{s+2} \qquad \text{as } y \to 0, \tag{D.1}$$

in place of (D.1). We will be interested in $s \neq 0$ and $n > 1$ (in fact $s$ will be determined precisely below for the main case of interest $n = 2$), so that the $x$ component of the momentum equation gives the restriction $c_{12}(x) = -c_{11}'(x)/(s+1)$ (assuming $s \neq -1$). Thus the equations (4.2) then give the solution

$$c_{11}(x) = k_1 c_0(x)^{\frac{(s+1)(s+2n)}{(s+2n-1)n}}, \qquad c_{12}(x) = -\frac{c_{11}'(x)}{(s+1)},$$

$$c_{22}(x) = c_{11}(x)\left(\frac{(s+2n)(s+2n+1)c_0'(x)^2}{n^2(s+2n-1)^2 c_0(x)^2} - \frac{c_0''(x)}{n(n-1)(s+2n-1)c_0(x)}\right),$$

where $K_1$ is an arbitrary constant of integration and $c_0(x)$ has to satisfy the third order nonlinear autonomous differential equation

$$c_0(x)^2 c_0'''(x) - \frac{(6n^2+3ns-5n-4s-2)}{n(s+2n-1)}c_0(x)c_0'(x)c_0''(x) - 2\frac{(n-1)^2(s+2n)(s+2n+1)}{n^2(s+2n-1)^2}c_0'(x)^3 = 0. \tag{D.2}$$

This is a constraint on admissible $c_0(x)$. For example, for algebraic behaviour $c_0(x) = C_0 x^{mn}$ where $C_0$ is an arbitrary constant the exponent $m$ can only take the values

$$m = 0, \quad m = \frac{(s+2n-1)}{(s+1)}, \quad m = \frac{(s+2n-1)}{(s+n)}.$$

Let us now impose $n = 2$, arguing that we are interested in flows from the outer core region that have a limiting wall shear rate. Due to (D.1), in place of (4.7) we take the more general inner scalings

$$x = X, \quad y = \delta Y, \quad \psi = \delta^2\Psi, \quad p = \bar{p}, \quad T_{11} = \delta^s\bar{T}_{11}, \quad T_{12} = \delta^{s+1}\bar{T}_{12}, \quad T_{22} = \delta^{s+2}\bar{T}_{22}, \tag{D.3}$$

where $\delta = \delta(\mathrm{We})$ will be determined. Ignoring inertia, the inner equations become

$$0 = -\frac{\partial\bar{p}}{\partial X} + \delta^s\left(\frac{\partial\bar{T}_{11}}{\partial X} + \frac{\partial\bar{T}_{12}}{\partial Y}\right), \tag{D.4}$$

$$0 = -\frac{\partial\bar{p}}{\partial Y} + \delta^{2+s}\left(\frac{\partial\bar{T}_{12}}{\partial X} + \frac{\partial\bar{T}_{22}}{\partial Y}\right), \tag{D.5}$$

$$\bar{T}_{11} + \delta\mathrm{We}\left(\frac{\partial\Psi}{\partial Y}\frac{\partial\bar{T}_{11}}{\partial X} - \frac{\partial\Psi}{\partial X}\frac{\partial\bar{T}_{11}}{\partial Y} - 2\frac{\partial^2\Psi}{\partial Y^2}\bar{T}_{12} - 2\frac{\partial^2\Psi}{\partial X\partial Y}\bar{T}_{11}\right)$$
$$+\hat{\kappa}\mathrm{We}^{1-r}\delta^s\bar{T}_{11}\left(\bar{T}_{11} + \delta\bar{T}_{12}\right) = 2\delta^{1-s}\frac{\partial^2\Psi}{\partial X\partial Y}, \tag{D.6}$$

$$\bar{T}_{22} + \delta\mathrm{We}\left(\frac{\partial\Psi}{\partial Y}\frac{\partial\bar{T}_{22}}{\partial X} - \frac{\partial\Psi}{\partial X}\frac{\partial\bar{T}_{22}}{\partial Y} + 2\frac{\partial^2\Psi}{\partial X^2}\bar{T}_{12} + 2\frac{\partial^2\Psi}{\partial X\partial Y}\bar{T}_{22}\right)$$
$$+\hat{\kappa}\mathrm{We}^{1-r}\delta^s\bar{T}_{22}\left(\bar{T}_{11} + \delta\bar{T}_{12}\right) = -2\delta^{-1-s}\frac{\partial^2\Psi}{\partial X\partial Y}, \tag{D.7}$$

$$\bar{T}_{12} + \delta\mathrm{We}\left(\frac{\partial\Psi}{\partial Y}\frac{\partial\bar{T}_{12}}{\partial X} - \frac{\partial\Psi}{\partial X}\frac{\partial\bar{T}_{12}}{\partial Y} + \frac{\partial^2\Psi}{\partial X^2}\bar{T}_{11} - \frac{\partial^2\Psi}{\partial Y^2}\bar{T}_{22}\right)$$
$$+\hat{\kappa}\mathrm{We}^{1-r}\delta^s\bar{T}_{12}\left(\bar{T}_{11} + \delta\bar{T}_{12}\right) = \delta^{-1-s}\left(\frac{\partial^2\Psi}{\partial Y^2} - \delta^2\frac{\partial^2\Psi}{\partial X^2}\right). \tag{D.8}$$

Balancing terms from the the upper convective stress derivative, quadratic stress and rate of strain terms gives

$$\delta\mathrm{We} = \mathrm{We}^{1-r}\delta^s = \delta^{-1-s}$$

and hence

$$s = \frac{(1-2r)}{(1+r)}, \qquad \delta = \mathrm{We}^{-\frac{1}{3}(1+r)}.$$

We thus obtain the equations (4.17)–(4.19) at leading order, and noting that $\delta^{2+s} = \mathrm{We}^{-1} \ll 1$, the momentum equation (D.5) gives

$$\bar{p} = \bar{p}_0(X) + O(\delta^{2+s}),$$

where $\bar{p}_0(X)$ is an arbitrary function of $X$. For $0 < r < 1/2$, we have $s > 0$ and thus (D.4) gives that $\bar{p}_0$ is a constant and thus at $O(\delta^s)$ we obtain the degenerate momentum equation

$$0 = \frac{\partial\bar{T}_{11}}{\partial X} + \frac{\partial\bar{T}_{12}}{\partial Y}. \tag{D.9}$$

The pressure gradient is recovered at leading order in the momentum equation at $r = 1/2$ i.e. $s = 0$ agreeing with the single layer structure result of section 4.1 that $r = 1/2$ when $n = 2$. For $r > 1/2$, $s < 0$ and (D.9) again persists. We note that the linear stress terms enter the leading order balance within (D.6)–(D.8) once $r = 2$. For $r > 2$ the quadratic stress terms are no longer present at leading order.

Thus our single layer structure cannot accomodate a general flow with an order one shear rate from the core outer solution for the full range of small $\kappa$. In general it severely restricts the possible shear rates $2c_0(x)$ it can accomodate through the requirement of $c_0(x)$ being a solution of (D.2) with $n = 2$. The only exception is when the pressure gradient is retained within the leading order boundary layer equations which occurs for $s = 0$ (equivalently $r = 1/2$ i.e. the case in the main text), so that the restriction (D.2) no longer applies. In some sense this is the reason why we shouldn't be surprised to see the two double layer structures, since they allow $n = 2$ and maintain the pressure gradient i.e. they make up for the defficiences of the single layer structure. This may be one of the most convincing arguments for their existence.